UCSF
UC San Francisco Electronic Theses and Dissertations

Title
Regulation of budding yeast morphogenesis by the Elm1 kinase

Permalink
https://escholarship.org/uc/item/5qg1b0v6

Author
Wei, Wei,

Publication Date
2003

Peer reviewed|Thesis/dissertation

eScholarship.org Powered by the California Digital Library
University of California

Regulation of budding yeast morphogenesis by the Elm1 kinase

by

WEI WEI

DISSERTATION

Submitted in partial satisfaction of the requirements for the degree of

DOCTOR OF PHILOSOPHY

in

Biochemistry and Molecular Biology

in the

GRADUATE DIVISION

of the

UNIVERSITY OF CALIFORNIA, SAN FRANCISCO

Aug. 24, 2004 Karen A. Butler

Date University Librarian

Degree Conferred:.....

ACKNOWLEGEMENTS

It is with a heavy heart writing up this thesis without the guidance of my principal investigator, Ira Herskowitz, who passed away in April 2003. I would like to thank him for providing constant encouragements throughout the years. I think he would be one of the happiest folk to see me finally graduate. Of all the scientists I have known, Ira is truly the one above the crowd. One of Ira's most admirable traits is his ability to teach. In fact, I consider myself lucky to attend UCSF at a time when he was still giving the Genetics lectures. He made the classes both fun and intellectually stimulating for the students. Another one of Ira's most admirable strengths is his ability to synthesize his thoughts from raw data. Ira was always the one to grasp the big picture while we were stuck in the details. I also have to thank Ira for attracting a great bunch of scientists in the lab and providing a nurturing environment for me to develop.

I would like to thank my former bay-mates Flora Banuett and Seiko Ishida for constant challenges and encouragements. I am especially grateful to Flora who started my graduate training by supervising my rotation in the lab. Later in graduate school I overlapped with a group of outgoing colleagues: Linda Huang, Kirsten Jaglo, Jun Urano, Emmitt Jolly, and Patrick Westfall. Their presence in the lab made the reality easier to deal with and life in the lab actually fun.

I had a group of recognizably smart scientists on my thesis committee, Pat O'Farrell, Dave Morgan, and Erin O'Shea. Looking back I wish I had made more contacts with them and learned more

from them during the early years in graduate school. Pat has always been a standout. When talking about science, it was almost expected that he would come up with a rather different perspective than the one I had. Thus I learned to keep an open mind when thinking about science. I am very grateful to Erin for not only providing scientific guidance but also for giving me a perching place in her lab to finish up.

Although I don't consider myself a gregarious person, I made several close friends in graduate school. Jen Whangbo and Javier Apfeld were instrumental in getting me attached to the world of board games. I also have lots of fond memories of the long biking trips past the Golden Gate Bridge when we used to be fit. Outside of school, I was happiest in the company of a group of friends I met through my favorite past-times, Badminton and hiking: Agnes Wong, Karin Wong, Chao Zhang, Darice Chan, Mimi Cheung, Horng Der Ou, Alex Wu, Richard Osman, and many others. I cannot imagine going through graduate school without their friendship and company.

Lastly I would like to thank my mom, sister, and dad for their unconditional love and unwavering support.

Abstract

Regulation of budding yeast morphogenesis by the Elm1 kinase

Wei Wei

Swe1, the budding yeast homologue of fission yeast wee1, is a protein kinase that can phosphorylate and inhibit some Cdc28-cyclin species *in vitro*. We have assayed tyrosine phosphorylation of Cdc28 as a monitor of Swe1 function to study its regulation *in vivo*. We observe that mutants defective in the *ELM1* gene exhibit increased Swe1-dependent tyrosine phosphorylation of Cdc28. The elongated-bud phenotype of *elm1* is partially suppressed by deleting *SWE1*. We find an increased level of Swe1 protein in *elm1* mutants. The half-life of Swe1 protein is increased to about four fold higher in *elm1* mutants than in wild-type cells. We find that moderate increase of Swe1 protein expression is sufficient to induce the elongated bud phenotype. We also find that Cdc28 Y-19 phosphorylation peaks in the G2 phase of the cell cycle when most of the Swe1 protein is turned over. Our results demonstrate that Elm1 is a negative regulator of Swe1 stability and that Swe1 protein expression needs to be tightly regulated in level and timing in budding yeast. To better understand Elm1 function we have studied the cellular localization of Elm1 protein. We find that Elm1 is localized specifically to the bud

neck and this localization is dependent on the septin ring integrity. We find that the C-terminal domain of Elm1 is necessary and sufficient for its localization to the bud neck. We find that like *elm1* mutants, septin mutants contain elevated levels of Swe1-dependent Cdc28 tyrosine 19 phosphorylation. We argue that Elm1 is involved in a bud morphogenesis checkpoint pathway that monitors the septin ring integrity.

Table of Contents

List of Figures

Chapter 1.

Introduction

Introduction

Budding yeast morphogenesis and the cell cycle

The cells of a uni-cellular organism and cells from an organ of a multi-cellular organism usually adopt specific shapes reflecting their living environments and their functionalities. For example, budding yeast cells are ovoid whereas fission yeast cells are cylindrical. The question why certain cells or cell types adopt certain shapes is subject to postulation and speculation. However, as a geneticist, one can answer the question how cell shapes are controlled genetically.

The yeast *Saccharomyces cerevisiae*, or budding yeast, is a model organism that can be used to study morphogenesis. The genome of the budding yeast was among the first to be completely sequenced (Goffeau et al., 1996). Genetic studies in budding yeast are further facilitated by the ease of genetic manipulation and the sophistication of research methods (Guthrie and Fink, 1991)

Budding yeast cells divide by the generation of a bud and its subsequent enlargement to a critical size before mitotic division. Morphogenesis in budding yeast therefore correlates intrinsically to the progression of the cell cycle. The sizes of the buds are often used an indication of which cell-cycle stage that active dividing yeast cells are in: unbudded cells are in the G1 phase; cells with a nascent bud indicate that they have just undergone the G1/S transition, or "START"; cells with small buds are in the S-phase; cells with large buds are in the G2/M phase. The growth phase of the bud has been

shown to undergo two steps: initial polar bud growth and later isotropic bud growth in G2 (for review, see Lew and Reed, 1995b).

The cell cycle progression in budding yeast is driven by a highly conserved cyclin-dependent protein kinase, Cdc28 (Beach et al., 1982). At various stages of the cell cycle, Cdc28 is complexed with specific sets of cyclins: during the G1 phase, Cdc28 is complexed with the G1 cyclins, Cln1, Cln2, and Cln3 (Hadwiger et al., 1989; Cross, 1988); during the S phase, Cdc28 is complexed with the S phase cyclins, Clb5 and Clb6 (Epstein and Cross, 1992; Kuhne and Linder, 1993); during the G2 phase, Cdc28 is complexed with the G2 cyclins, Clb1 and Clb2 (Surana et al., 1991). Cdc28 kinase activity is also regulated by other mechanisms besides its activation via association with the cyclins. Full activation of Cdc28 kinase activity requires phosphorylation of Cdc28 threonine 169 by the Cak1 kinase (Espinoza et al., 1996; Kaldis et al., 1996). In addition, the Swe1 kinase inhibits Cdc28 kinase activity via phosphorylation of Cdc28 tyrosine 19 (Booher et al., 1993). These three modes of regulation of Cdc28 kinase activity are conserved from the yeast to mammals.

With its fundamental role in the regulation of the nuclear division, perhaps it is not surprising that Cdc28 is involved in the regulation of budding yeast morphogenesis. Mutations in the *CDC28* gene and in its regulators have been reported that result in altered morphology. Numerous observations demonstrate that elevated levels of the G1 cyclin-Cdc28 activity, or reduced levels of the G2 cyclin-Cdc28 activity lead to elongated bud morphology (Lew and Reed, 1993; Blacketer et al., 1995; Ahn et al., 1999; Ahn et al., 2001). The direct targets of Cdc28 kinase in the regulation of bud morphogenesis however remain elusive.

The role of Swe1 in budding yeast morphogenesis

Particular attention should be given to the function of Swe1 kinase in studying the regulation of budding yeast morphogenesis. Overexpression of Swe1 results in highly elongated buds (Booher et al., 1993). On the other hand, mutations in the *SWE1* gene suppress a large number of mutants that exhibit elongated bud morphology (Ma et al., 1996; Altman and Kellogg, 1997; Longtine et al., 1998; Barral et al., 1999). Swe1 is protein kinase of 819 amino acids that inhibits the Cdc28 kinase activity via phosphorylation of Cdc28 tyrosine 19 (Booher et al., 1993). Swe1 phosphorylates Cdc28 complexed with the G2 cyclins, but not that complexed with the G1 cyclins, thereby demonstrating substrate specificity (Booher et al., 1993). Swe1 shows significant identity to its homolog in fission yeast, wee1, in the kinase domain (Booher et al., 1993). In fission yeast wee1 is negatively regulated by the nim1 protein kinase (Russell and Nurse, 1987; Wu and Russell, 1993). Three nim1 kinase homologs exist in budding yeast, Hsl1, Gin4, and Kcc4 (Ma et al., 1996; Altman and Kellogg, 1997; Longtine et al., 1998). Mutations in *HSL1* and in *GIN4* result in elongated bud morphology. Even though it has not been established biochemically whether Swe1 is a substrate for the nim1 homologs in budding yeast, the elongated bud morphology of *hsl1* and *gin4* mutants required an intact *SWE1* gene (Ma et al., 1996; Altman and Kellogg, 1997; Longtine et al., 1998; Barral et al., 1999). In addition, Swe1 has been localized to the bud neck and to the nucleus. Its localization to the bud neck is dependent on Hsl1 (Longtine et al.,

2000). Regulation of Swe1 by the nim1 homologs also occurs at the level of Swe1 protein stability. It has been demonstrated that Swe1 protein degradation requires Hsl1 (McMillan et al., 1999).

Morphogenesis checkpoints that regulate Swe1

The nim1 homologs are localized to the bud neck in a septin-dependent manner (Okuzaki et al., 1997; Longtine et al., 1998; Barral et al., 1999). A morphogenesis checkpoint mechanism that monitors the septin ring integrity has been suggested that coordinates the septin ring assembly and cell cycle progression (Barral et al., 1999). Septins are a family of GTP-binding proteins that form into a ring of 10-nm filaments at the bud neck. Members of the septins, Cdc3, Cdc10, Cdc11, Cdc12, and Sep7 have been localized to the bud neck (Byers and Goetsch, 1976; Ford and Pringle, 1991; Kim et al., 1991; Frazier et al., 1998). Septin mutants exhibit elongated bud phenotypes that are suppressed by a *swe1* mutation (Barral et al., 1999). However, septins have an essential function that is independent of *SWE1*, as the temperature-sensitive phenotype of some septin mutants is not rescued by a *swe1* deletion. It has been suggested that the septin ring at the bud neck acts as a diffusion barrier between the mother and the bud (Barral et al., 2000).

A morphogenetic checkpoint that monitors the bud formation and actin cytoskeleton assembly has also been described (Lew and Reed, 1995a; McMillan et al., 1998). It is shown that perturbation of the bud formation or disruption of the actin cytoskeleton result in a *SWE1*-dependent delay in nuclear division.

Study of Elm1 regulation of Swe1 in yeast morphogenesis

ELM1 was identified in a screen for morphogenetic mutants in budding yeast (Blacketer et al., 1993). *ELM1* encodes a serine, threonine protein kinase of 640 amino acids in budding yeast (Blacketer et al., 1993; Koehler et al., 1997). Mutants of *elm1* strains exhibit an elongated bud phenotype that is suppressed by a *swe1* mutation (Edgington et al., 1999), thereby suggesting that *ELM1* negatively regulates *SWE1*.

We have independently identified *ELM1* in a screen for mutants that are defective in the switch from polar to isotropic bud growth. We have carried out biochemical and cell biological experiments to understand the regulation of Swe1 by Elm1. We find that Elm1 is required for the down-regulation of Swe1 protein level, and its kinase activity. We observe that Elm1 is localized to the bud neck. We find that localization of Elm1 to bud neck is mediated via its C-terminal domain and is dependent on the integrity of the septins. We argue that Elm1 is involved in a morphogenesis checkpoint that monitors the septin ring integrity.

References

Ahn, S.H., A. Acurio, and S.J. Kron. 1999. Regulation of G2/M progression by the STE mitogen-activated protein kinase pathway in budding yeast filamentous growth. *Mol. Biol. Cell* **10**: 3301-16.

Ahn, S.H., B.T. Tobe, J.N. Fitz Gerald, S.L. Anderson, A. Acurio, and S.J. Kron. 2001. Enhanced cell polarity in mutants of the budding yeast cyclin-dependent kinase Cdc28p. *Mol. Biol. Cell* **12**: 3589-600.

Altman, R. and D. Kellogg. 1997. Control of mitotic events by Nap1 and the Gin4 kinase. *J. Cell Biol.* **138**: 119-130.

Barral, Y., V. Mermall, M.S. Mooseker, and M. Snyder. 2000. Compartmentalization of the cell cortex by septins is required for maintenance of cell polarity in yeast. *Mol. Cell* **5**: 841-51.

Barral, Y., M. Parra, S. Bidlingmaier, and M. Snyder. 1999. Nim1-related kinases coordinate cell cycle progression with the organization of the peripheral cytoskeleton in yeast. *Genes & Dev.* **13**: 176-187.

Beach, D., B. Durkacz, and P. Nurse. 1982. Functionally homologous cell cycle control genes in budding and fission yeast. *Nature* **300**: 706-9.

Blacketer, M.J., C.M. Koehler, S.G. Coats, A.M. Myers, and P. Madaule. 1993. Regulation of dimorphism in *Saccharomyces cerevisiae*: involvement of the novel protein kinase homolog Elm1p and protein phosphatase 2A. *Mol. Cell. Biol.* **13**: 5567-5581.

Blacketer M.J., P. Madaule, and A.M. Myers. 1995. Mutational analysis of morphologic differentiation in *Saccharomyces cerevisiae*. *Genetics* **140**: 1259-1275.

Booher, R.N., R.J. Deshaies, and M.W. Kirschner. 1993. Properties of *Saccharomyces cerevisiae* wee1 and its differential regulation of $p34^{CDC28}$ in response to G1 and G2 cyclins. *EMBO J.* **12**: 3417-3426.

Byers, B. and L. Goetsch. 1976. A highly ordered ring of membrane associated filaments in budding yeast. *J. Cell Biol.* **69**: 717-721.

Cross, F.R. 1988. *DAF1*, a mutant gene affecting size control, pheromone arrest, and cell cycle kinetics of *Saccharomyces cerevisiae*. *Mol. Cell. Biol.* **8**: 4675-84.

Edgington, N. P., M. J. Blacketer, T. A. Bierwagen, and A. M. Myers. 1999. Control of *Saccharomyces cerevisiae* filamentous growth by cyclin-dependent kinase Cdc28. *Mol. Cell. Biol.* **19**: 1369-1380.

Epstein, C.B. and F.R. Cross. 1992. *CLB5*: a novel B cyclin from budding yeast with a role in S phase. *Genes Dev.* **6**: 1695-706.

Espinoza, F.H., A. Farrell, H. Erdjument-Bromage, P. Tempst, and

D.O. Morgan. 1996. A cyclin-dependent kinase-activating kinase (CAK) in budding yeast unrelated to vertebrate CAK. *Science* **273**: 1714-7.

Ford, S.K. and J.R. Pringle. 1991. Cellular morphogenesis in the *Saccharomyces cerevisiae* cell cycle: localization of the *CDC11* gene product and the timing of events at the budding site. *Dev. Genet.* **12:** 281-292.

Frazier, J.A., M.L. Wong, M.S. Longtine, J.R. Pringle, M. Mann, T.J. Mitchison, and C. Field. 1998. Polymerization of purified yeast septins: evidence that organized filament arrays may not be required for septin function. *J. Cell Biol.* **143**: 737-749.

Goffeau, A. *et al.* 1996. Life with 6000 genes. *Science* **274**: 563-567.

Guthrie, C. and G.R. Fink. 1991. Guide to yeast genetics and molecular biology. *Meth. Enzymol.* **194**: 1-933.

Hadwiger, J.A., C. Wittenberg, H.E. Richardson, M. de Barros Lopes, and S.I. Reed. 1989. A family of cyclin homologs that control the G1 phase in yeast. *Proc. Natl. Acad. Sci.* **86**: 6255-9.

Kaldis, P., A. Sutton, M.J. Solomon. 1996. The Cdk-activating kinase (CAK) from budding yeast. *Cell* **86**: 553-64.

Kim, H.B., B.K. Haarer, and J.R. Pringle. 1991. Cellular morphogenesis in the *Saccharomyces cerevisiae* cell cycle: localization

of the *CDC3* gene product and the timing of events at the budding site. *J. Cell Biol.* **112**: 535-544.

Kuhne, C. and P. Linder. 1993. A new pair of B-type cyclins from *Saccharomyces cerevisiae* that function early in the cell cycle. *EMBO J.* **12**: 3437-47.

Lew, D.J. and S.I. Reed. 1993. Morphogenesis in the yeast cell cycle: Regulation by Cdc28 and cyclins. *J. Cell Biol.* **120**: 1305-1320.

Lew, D.J. and S.I. Reed. 1995a. A cell cycle checkpoint monitors cell morphogenesis in budding yeast. *J. Cell Biol.* **129**: 739-749.

Lew, D.J. and S.I. Reed. 1995b. Cell cycle control of morphogenesis in budding yeast. *Curr. Opin. Genet. Dev.* **5**: 17-23.

Longtine, M.S., H. Fares, and J.R. Pringle. 1998. Role of the yeast Gin4p and the relationship between septin assembly and septin function. *J. Cell Biol.* **143**: 719-736.

Longtine, M.S., C.L. Theesfeld, J.N. McMillan, E. Weaver, J.R. Pringle, and D.J. Lew. 2000. Septin-dependent assembly of a cell cycle-regulatory module in *Saccharomyces cerevisiae*. *Mol. Cell. Biol.* **20**: 4049-61.

Ma, X.-J., Q. Lu, and M. Grunstein. 1996. A search for proteins that interact genetically with histone H3 and H4 amino termini uncovers

novel regulators of the Swe1 kinase in *Saccharomyces cerevisiae*. *Genes & Dev.* **10**: 1327-1340.

McMillan, J.N., R.A. Sia, and D.J. Lew. 1998. A morphogenesis checkpoint monitors the actin cytoskeleton in yeast. *J Cell Biol.* **142**: 1487-99.

McMillan, J.N., M.S. Longtine, R.A.L. Sia, C.L. Theesfeld, E.S.G. Bardes, J.R. Pringle, and D.J. Lew. 1999. The morphogenesis checkpoint in *Saccharomyces cerevisiae* : cell cycle control of Swe1p degradation by Hsl1p and Hsl7p. *Mol. Cell. Biol.* **19**: 6929-6939.

Okuzaki, D., S. Tanaka, H. Kanazawa, and H. Nojima. 1997. Gin4 of *S. cerevisiae* is a bud neck protein that interacts with the Cdc28 complex. *Genes Cells.* **2**: 753-770.

Russell, P. and P. Nurse. 1987. The mitotic inducer nim1 functions in a regulatory network of protein kinase homologs controlling the initiation of mitosis. *Cell* **49**: 569-576.

Surana, U., H. Robitsch, C. Price, T. Schuster, I. Fitch, B. Futcher, and K. Nasmyth. 1991. The role of CDC28 and cyclins during mitosis in the budding yeast *S. cerevisiae*. *Cell* **65**: 145-61.

Wu, L. and P. Russell. 1993. Nim1 kinase promotes mitosis by inactivating wee1 tyrosine kinase. *Nature* **363**: 738-741.

Chapter 2.

Regulation of the Cdk inhibitory kinase Swe1 by the Elm1 kinase in budding yeast morphogenesis

Regulation of the Cdk inhibitory kinase Swe1 by the Elm1 kinase in budding yeast morphogenesis

Wei Wei and Ira Herskowitz

Department of Biochemistry and Biophysics
University of California, San Francisco
San Francisco, CA 94143-0448

[*Key Words*: Elm1; Swe1; Cdc28 tyrosine phosphorylation; morphogenesis; cell cycle]

For proofs and editorial correspondence, please contact:

Wei Wei
Email: weiwei@itsa.ucsf.edu

Abstract

Swe1, the budding yeast homologue of fission yeast wee1, is a protein kinase that can phosphorylate and inhibit some Cdc28-cyclin species *in vitro*. We have assayed tyrosine phosphorylation of Cdc28 as a monitor of Swe1 function to study its regulation *in vivo*. We observe that mutants defective in the *ELM1* gene exhibit increased Swe1-dependent tyrosine phosphorylation of Cdc28. The elongated-bud phenotype of *elm1* is partially suppressed by deleting *SWE1*. We find an increased level of Swe1 protein in *elm1* mutants. The half-life of Swe1 protein is increased to about four fold higher in *elm1* mutants than in wild-type cells. We find that moderate increase of Swe1 protein expression is sufficient to induce the elongated bud phenotype. We also find that Cdc28 Y-19 phosphorylation peaks in the G2 phase of the cell cycle when most of the Swe1 protein is turned over. Our results demonstrate that Elm1 is a negative regulator of Swe1 stability and that Swe1 protein expression needs to be tightly regulated in level and timing in budding yeast.

Introduction

The activity of cyclin-dependent kinases is under a variety of controls, for example, inhibitory phosphorylation by protein kinases such as wee1 in fission yeast and its human homologue (Russell and Nurse, 1987a; Parker et al., 1995). In *S. pombe*, wee1 inhibits the cyclin-dependent kinase cdc2 by phosphorylating the tyrosine 15 residue of cdc2. Phosphorylation by wee1 regulates the size at which fission yeast cells enter mitosis and mediates cell cycle arrest in response to DNA damage or incomplete DNA replication (Rhind et al., 1997; Enoch and Nurse, 1990). Activity of wee1 is negatively regulated by the kinase nim1, which phosphorylates the kinase domain of wee1 (Russell and Nurse, 1987b; Parker et al., 1993; Wu and Russell, 1993). Budding yeast contains homologues of these proteins: the cdc2 homologue, Cdc28; the wee1 homologue, Swe1; and three nim1 homologues, Hsl1, Gin4, and Kcc4 (Russell et al., 1989; Ma et al., 1996; Altman and Kellogg, 1997; Longtine et al., 1998b; Barral et al., 1999).

Swe1 has been identified through its sequence homology with wee1 (Booher et al., 1993). *In vitro* studies demonstrate that Swe1 can phosphorylate Cdc28, presumably on the tyrosine 19 residue, and inhibit its histone H1 kinase activity (Booher et al., 1993). Swe1 inhibitory phosphorylation on Cdc28 exhibits specificity in that Swe1 is capable of phosphorylating Cdc28 complexed with a G2 cyclin, but not that complexed with a G1 cyclin. Unlike deletion of *wee1* in fission yeast, which leads to a Wee phenotype (cytokinesis at small cell size), deletion of *SWE1* does not have immediate observable

effect on budding yeast cell cycle progression or cell shape (Booher et al., 1993). *SWE1* also does not participate in the DNA damage checkpoint or in monitoring incomplete DNA replication. Similarly, mutating the Swe1 phosphorylation site in Cdc28 from tyrosine 19 to phenylalanine does not affect any of these processes (Sorger and Murray, 1992; Amon et al., 1992). However, a careful comparison of the daughter cell volume between *swe1* and wild-type cells does show a smaller size in *swe1* daughter cells (Harvey and Kellogg, 2003). Thus it appears that *SWE1* is involved in a conserved mechanism that controls cell size during mitosis in budding yeast. In addition, *SWE1* can be seen to affect budding yeast *in vivo* under the following circumstances. First, overexpression of Swe1 leads to a G2 delay and the formation of elongated buds (Booher et al., 1993). Second, deletion of *SWE1* relieves the G2 delay observed in mutants lacking the phosphatase, Mih1, which removes the phosphate added by Swe1 (Booher et al., 1993). Third, deletion of *SWE1* suppresses the G2 delay and elongated-bud phenotype of *hsl1* and *hsl7* mutants (Ma et al., 1996; Barral et al., 1999) and of *elm1* mutants (Edgington et al., 1999; Sreenivasan and Kellogg, 1999; Bouquin et al., 2000). Fourth, *SWE1* appears to be responsible for a morphogenetic checkpoint, in which nuclear division is delayed in cells that are defective in bud emergence or whose actin cytoskeleton is perturbed (Lew and Reed, 1995a; Sia et al., 1996). Fifth, *SWE1* appears to be involved in a bud morphogenesis checkpoint that coordinates the cell cycle progression with the septin ring assembly at the bud neck (Barral et al., 1999). These actions of *SWE1* are interpreted as the result of Swe1 phosphorylation of Cdc28 tyrosine 19. For example, a *cdc28Y19F* mutation has been shown to reverse the effect of Swe1

overexpression (Booher et al., 1993), whereas a *cdc28Y19E* mutation has been shown to mimic Swe1 overexpression (Lim et al., 1996).

Growth of a yeast bud switches from apical to isotropic in order to produce an ovoid cell shape (reviewed by Lew and Reed, 1995b). After initiation of bud formation at Start, growth of the bud is polarized towards the bud tip while the bud is small. This is the period of apical bud growth. At a certain point in G2, growth of the bud becomes uniformly distributed over its surface, i.e., isotropic. A variety of observations indicate that Cdc28 associated with G1 cyclins such as Cln2 promotes apical bud growth and that Cdc28 associated with G2 cyclins such as Clb2 promotes isotropic bud growth (Lew and Reed, 1993; Ahn et al., 1999; Ahn et al., 2001).

A number of mutants that form elongated buds have identified genes that may play a role in the switch from apical to isotropic growth (Blacketer et al., 1995; Kellogg and Murray, 1995; Altman and Kellogg, 1997). In particular, Myers and colleagues have found mutations in fourteen genes that give an elongated-bud phenotype. One of these is the *ELM1* gene, which encodes a protein kinase (Blacketer et al., 1993; Koehler and Myers, 1997). It is subsequently shown that mutations in the *SWE1* gene suppress the elongated-bud phenotype of *elm1* cells therefore suggesting that *ELM1* negatively regulates *SWE1* (Edgington et al., 1999; Sreenivasan and Kellogg, 1999). In addition, it has been observed that the electrophoretic mobility of Swe1 is affected in *elm1* mutants presumably reflecting reduced phosphorylation of Swe1 (Sreenivasan and Kellogg, 1999). We have identified *ELM1* in a genetic screen for mutants defective in the switch from polar to isotropic bud growth. We have carried out biochemical and cell biological experiments in order to understand

the regulation of *SWE1* by *ELM1*. We show that Elm1 is involved in the regulation of protein stability of Swe1. We also show that moderate over-expression of Swe1 is sufficient to induce elongated-bud morphology, thereby mimicking *elm1* phenotype. We find that even though Swe1 protein expression peaks in the S phase of the cell cycle, its kinase activity peaks later in the G2 phase of the cell cycle, suggesting a potential role of Swe1 in guarding against premature activation of the Cdc28-Clb2 activity. We find that *elm1* mutants exhibit prolonged tyrosine 19 phosphorylation on Cdc28 in G2, suggesting that *ELM1* is required for the timely down-regulation of *SWE1* activity.

Materials and methods

DNA manipulations, yeast strains, and media

Yeast strains used in this study are listed in Table 1. Yeast growth media and genetic manipulations were as described (Guthrie and Fink, 1991). DNA manipulations are as described in Sambrook et al. (1989).

ELM1 deletion strain

A 3.4 kb XbaI fragment of the genomic sequence containing the *ELM1* gene was cloned in plasmid pRS306 (Sikorski and Hieter, 1989). The plasmid was cut with HpaI, releasing most of the *ELM1* ORF. The 6.0 kb fragment containing the pRS306 backbone and the 5′ and 3′ flanking region of the *ELM1* ORF was ligated to a 1.1 kb *TRP1* fragment, resulting in a plasmid in which the *ELM1* ORF was replaced by *TRP1*. The resulting *elm1Δ::TRP1* plasmid was cut with ClaI to target the disruption of the *ELM1* gene in the yeast genome.

SWE1 *deletion strains*

To obtain *swe1Δ::LEU2* strains, the plasmid pSWE1-10g (Booher et al., 1993) was cut with HindIII and BamHI and used in yeast transformations.

Table 1. Yeast strains used.

Strain	Relevant Genotype	Origin
yWW001	*MATa ade2-1 trp1-1 can1-100 leu2-3,112 his3-11,15 ura3-1*	IH collection[a]
yWW018	*MATα ade2-1 trp1-1 can1-100 leu2-3,112 his3-11,15 ura3-1*	IH collection[a]
yWW067	*MATa leu2::P_{GAL1}::CLN3-2::LEU2::URA3*	This study[a]
yWW069	*MATa leu2::P_{GAL1}::CLN3-2::LEU2::URA3 elm1*	This study[a]
yWW274	*MATa elm1::TRP1*	This study[a]
yWW447	*MATa elm1::TRP1 swe1::LEU2*	This study[a]
yWW026	*MATa swe1::LEU2*	This study[a]
yWW336	*MATa CDC28-HA::URA3*	Rudner and Murray[a]
yWW338	*MATa CDC28VF-HA::URA3*	Rudner and Murray[a]
yWW667	*MATa elm1::TRP1 CDC28-HA::URA3*	This study[a]
yWW659	*MATa swe1::LEU2 CDC28-HA::URA3*	This study[a]
yWW669	*MATa elm1::TRP1 swe1::LEU2 CDC28-HA::URA3*	This study[a]
yWW657	*MATa elm1::TRP1 cdc28VF-HA::URA3*	This study[a]
yWW612	*MATa SWE1-myc_{13}::his5+*	This study[a]
yWW613	*MATa SWE1-myc_{13}::his5+ elm1::TRP1*	This study[a]
yWW648	*MATa swe1::TRP1::P_{GAL1}::SWE1::myc_{13}::his5+*	This study[a]
yWW684	*MATa swe1::TRP1::P_{GAL1}::SWE1::myc_{13}::his5+ elm1::URA3*	This study[a]
yWW951	*MATa swe1::hisG pRS316*	This study[a]
yWW952	*MATa swe1::hisG pRS316-SWE1*	This study[a]
yWW954	*MATa swe1::hisG elm1::TRP1 pRS316-SWE1*	This study[a]
yWW953	*MATa swe1::hisG pRS313-SWE1 pRS314-SWE1 pRS315-SWE1 pRS316-SWE1*	This study[a]
yWW703	*MATa/MATα CLN2/CLN2-HA::LEU2 CDC28/CDC28-HA::URA3 SWE1/SWE1-myc_{13}::his5+ ELM1/elm1::TRP1*	This study[a]

a. Strains are in the W303 background

To obtains *swe1Δ::hisG* strains, a pair of primers 5'-TTGCGTAGTGCTGGGGAAAAGTAAACACACACAGGCGCACACGAGAACAGCACAGGAAACAGCTATGACC-3' and 5'-ACAAGGTTTTTTGTTCCATTTATCATATAAAAAATTTTGGCTTAGGTCCAGTTGTAAAACGACGGCCAGT-3' were used in a PCR reaction using the plasmid pCgTRP1 as template (Kenji Irie). The resulting PCR product was used in yeast transformations to obtain *swe1Δ::TRP1* strain. A ptrp1ΔhisG-URA3-hisG (CY567) plasmid was linearized and used to transform *swe1Δ::TRP1* strains to obtain *swe1Δ:::hisG::URA3::hisG* strain. The *swe1Δ::hisG* strains were obtained by selection of cells that carried out spontaneous loop-out of the *URA3* marker using plates containing the drug 5FOA.

SWE1::myc13::his5^{+} *strains*

The *SWE1::myc13::his5*$^{+}$ strain was constructed using the one-step gene tagging method as described (Longtine et al., 1998a). Plasmid pFA6a-13Myc-His3MX6 (Longtine et al., 1998a) was used as template for PCR reaction using primers 5′-GTGCTATTATCCAGGAAGACGACTTTGGACCTAAGCCAAAATTTTTATACGGATCCCCGGGTTAATTAA-3′, and 5′-ACGTGTGGGAAAAAAGTATGTAAATAAAACAAGGTTTTTTGTTCCATTTAGAATTCGAGCTCGTTTAAAC-3′. The PCR product was used in yeast transformations to obtain *SWE1::myc13::his5*$^{+}$ strains.

Yeast extract preparation for immunoprecipitations

Cells were grown to exponential phase (OD_{600} ca. 0.8). For each immunoprecipitation reaction, 50 ml of yeast culture was pelleted. All subsequent manipulations were carried out at 4°C. To the cell pellet, 0.5 ml glass beads and 0.6 ml lysis buffer (50 mM Tris [pH 7.5], 1 mM EDTA, 100 mM NaCl, 0.1% NP-40, 10 mM NaF, 50 mM β-glycerolphosphate, 0.1 mM Na_3VO_4, and 1 tablet of protease inhibitor cocktail [Amersham]) were added. The contents were vigorously homogenized with a multi-beadbeater (BioSpec Products) for four 1 min periods. Glass beads and cell debris were pelleted by centrifugation, and the crude extract clarified by three 10 min microfuge spins. Protein concentration of the yeast extract was measured using the Bio-Rad protein assay. Yeast extracts from various strains were adjusted to the same protein concentration using lysis buffer.

Whole-cell lysates

1.5 ml of yeast culture at OD_{600} ca. 0.7 was pelleted and resuspended in 150 μl 1 M NaOH, 0.074% β-mercaptoethanol for 10 min at 4°C. 150 μl 50% w/v trichloroacetic acid (TCA) was added and incubated for 10 min at 4°C. The contents were spun for 2 min in a microfuge at 4°C, and the pellet was washed with 1 ml ice-cold acetone. After a short microfuge spin, acetone was removed and 150 μl of SDS-PAGE

sample buffer was added. Contents were boiled for 5 min before loading on SDS-PAGE mini-gels.

Immunoprecipitation

12CA5 HA monoclonal antibody was cross-linked to protein A-Sepharose beads (Harlow and Lane, 1989) with a ratio of 2 μl antibody per 40 μl beads. 40 μl of coupled beads was added to yeast extracts of the same volume and of the same protein concentration from various strains. After incubation at 4°C with gentle shaking for 2 hours, the beads were pelleted, washed three times with lysis buffer, and resuspended in 150 μl SDS-PAGE sample buffer. Alternatively, 12CA5 affinity matrix (Covance Research Products) was used in HA immunoprecipitation experiments.

Polyacylamide gel electrophoresis and Western blotting

Samples were fractionated using 10% SDS-polyacrylamide mini-gels. Proteins were transferred to nitrocellulose filters in transfer buffer (0.2 M glycine, 0.03 M Tris, 0.1% SDS, 20% methanol). Filters were blocked for 1 hour in phosphate-buffered saline (PBS; 137 mM NaCl, 2.7 mM KCl, 8.1 mM Na_2HPO_4, 1.5 mM KH_2PO_4 [pH 7.2]) containing 0.1% Triton X-100 and 2% nonfat dry milk. 12CA5 HA monoclonal antibody (Berkeley Antibody Company), phosphotyrosine antibody (Transduction Laboratories), phospho-cdc2 antibody (kindly provided by NEB Biolabs), myc monoclonal antibody (Berkeley

Antibody Company), Ste12 antibody (kindly provided by Mary Maxon), or Swe1 antibody (kindly provided by Douglas Kellogg) was added at the recommended concentrations. Antigen was visualized using the Amersham ECL detection kit.

Stripping of Western blots

Filters were stripped of previously applied antibodies by immersing in stripping buffer (62.5 mM Tris [pH 6.8], 2% SDS, 100 mM β-mercaptoethanol) at 70°C for 30 min, and washed extensively in PBS.

Quantitation of Cdc28-HA tyrosine phosphorylation

To ensure that we immunoprecipited the same amount of Cdc28-HA protein, yeast extracts of the same volume and of the same protein concentration from various strains were prepared. To compare the relative amount of tyrosine phosphorylation in two strains, Cdc28-HA immunoprecipitates from strains exhibiting higher tyrosine phosphorylation, i.e., the *elm1Δ* strain or *cdc12-6* strain, were diluted serially. The dilution that exhibited the same level of tyrosine phosphorylation with the reference, i.e., wild-type strain, determined the fold difference between the two strains.

Determination of Swe1 stability

Cells containing the P_{GAL1}::*SWE1*::*myc13* construct were grown in raffinose meidum to early log phase. Galactose was added to 2% and cells were incubated for 15 minutes to induce Swe1-myc$_{13}$ protein expression. Cells were then harvested and resuspened at 10^8 density in labeling medium (raffinose medium supplemented with 2% galactose and 0.25 mCi/ml of [S-35]methionine (Amersham) for 10 minutes. Labeled cells were collected by filtration through a Nalgene filter, washed with YEPD and resuspended in YEPD supplemented with 3mM methionine. Aliquots of the culture were collected at the indicated time-points by centrifugation and frozen at -20°C. To determine Swe1 stability in synchronized cultures, cells were treated with 10μM nocodazole for 2 hours prior to the addition of galactose to the media and 10μM nocodazole was included in the media thereafter. Cell pellets were lysed in ice-cold lysis buffer (50 mM Tris [pH 7.5], 1 mM EDTA, 150 mM NaCl, 1% NP-40, 10 mM NaF, 50 mM β-glycerolphosphate, 0.1 mM Na_3VO_4, and 1 tablet of protease cocktail [Amersham]) on a Mini-BeadBeater-8 [BioSpec Products]). The specific activities of the lysates were quantitated using a liquid scintillation counter and normalized. Swe1-myc13 protein was immunoprecipitated with the 9E10 affinity matrix (Covance Research Products) from lysates of the same amount of radioactive label and of the same volume. The immunoprecipitates were washed three times with lysis buffer, boiled in 1X SDS sample buffer, and separated on a 7.5% SDS-PAGE mini-gel. Dried gels were exposed to a PhosphorImager screen (Molecular Dynamics) and analyzed with ImageQuant software.

Photography and image processing

For morphological studies, cells were visualized with a Zeiss Axioskop and photographed with Polaroid film. Images were processed using Adobe Photoshop software.

Results

Identification of ELM1 *in a screen for mutants defective in the switch from polar to isotropic bud growth*

We were interested in the genes in budding yeast that regulate the switch from polar to isotropic bud growth. Since it has been observed that the G1 cyclins promote polar bud growth, we reasoned that mutants defective in the switch might not tolerate hyper-activation of the G1 cyclins. A yeast strain yWW067 was constructed in which a hyper-stable allele of *CLN3*, *CLN3-2* was expressed under the transcriptional control of a *GAL1* promoter. We found that when grown in YEP glucose medium, yWW067 cells exhibited wild-type morphology and showed wild-type cell-cycle progression profile when examined by FACS; when they were grown in YEP galactose medium, yWW067 cells exhibited phenotypes such as smaller cell size, alpha mating factor resistance, and accumulation of G2 population which are consistent with the expression of *CLN3-2* (data not shown; Cross 1988). This strain was mutagenized with UV irradiation and mutants that could not grow on YEP galactose medium were isolated. One of the isolated mutants, yWW069 exhibited elongated bud phenotype on YEP glucose medium (Figure 1). They exhibited a growth defect with strikingly elongated bud morphology on YEP galactose medium when *CLN3-2* was over-expressed from the *GAL1* promoter (Figure 1). Standard tetrad analysis showed that the elongated bud phenotype was due to a single gene trait. Plasmids from a cen-ars yeast genomic library were

used to rescue the elongated bud morphology on YEP glucose medium. Sequences of two independent and complementing plasmids showed that they both carried the *ELM1* gene. Deletion of the *ELM1* gene in these plasmids resulted in failure to complement the mutant phenotype. Deletion of the *ELM1* gene in yeasts with otherwise wild-type genetic background resulted in mutants that showed elongated bud phenotype. We also found that a cen-ars *ELM1* plasmid was able to complement the growth defect and the elongated bud morphology of yWW069 cells on YEP galactose medium. We therefore conclude that mutations in the *ELM1* gene are responsible for the elongated bud mutant phenotype and that mutations in the *ELM1* gene exhibit synthetic interactions with over-expression of hyper-stable alleles of *CLN3*.

Edgington et al. (1999) have observed that mutations in the *SWE1* gene suppressed the elongated bud phenotype of *elm1* mutants. In order to determine whether the behavior of *elm1* mutants is due to hyperactive *SWE1*, we set out to confirm their observation. An *elm1Δ swe1Δ* strain was constructed by crossing the two single mutants. Isogenic wild-type and *swe1Δ* strains exhibited normal morphology; the *elm1Δ* strain formed chains of elongated cells. In contrast, the *elm1Δ swe1Δ* strain formed cells of near wild-type morphology. These cells remained attached as in the *elm1Δ SWE1* strain. Thus we confirmed that the elongated bud phenotype of the *elm1Δ* strain requires *SWE1* (data not shown).

Figure 1. Mutations in the *ELM1* gene show synthetic interaction with a hyperactive allele of G1 cyclin. Wild-type stain yWW001 and *elm1* P_{GAL1}-*CLN3-2* strain yWW069 were grown in raffinose medium to exponential phase. Galactose was added to the cultures for 4 hours and cellular morphology was observed using Nomarski optics.

Figure 1

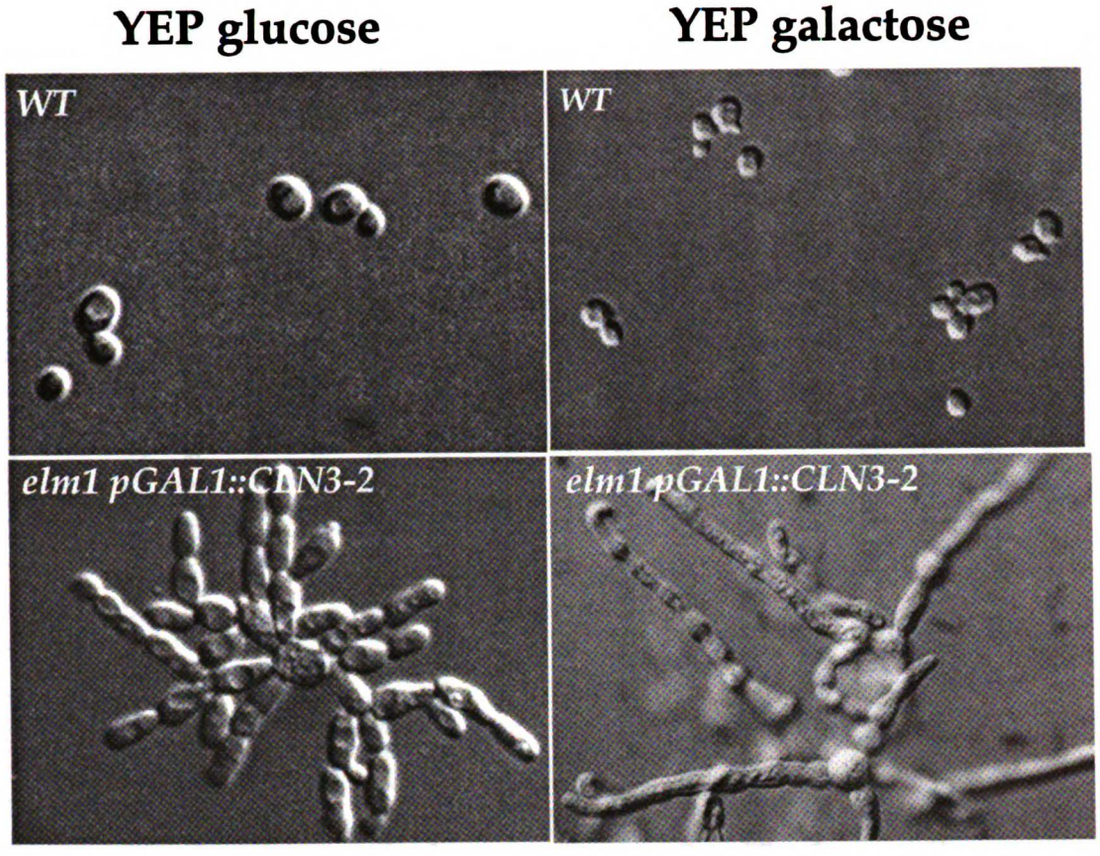

UCSF LIBRARY

elm1 *mutants exhibit elevated levels of Cdc28 Y-19 phosphorylation*

In order to determine whether the behavior of *elm1* mutants is due to possible hyperactive Swe1 kinase activity, we monitored the level of tyrosine phosphorylation on Cdc28 in *elm1* mutants, using phosphotyrosine antibody to analyze immunoprecipitated Cdc28 (Figure 2A, see Materials and methods). A no tag control experiment was carried out to demonstrate the specificity of immunoprecipitation procedure using 12CA5 antibody (Figure 2A, lane 1). Wild-type cells exhibited a basal level of tyrosine phosphorylation (Figure 2A, lane 2). This phosphorylation was absent in strains deleted for *SWE1* (Figure 2A, lane 4) or with the *cdc28V18F19* mutation (Figure 2A, lane 6), indicating that tyrosine phosphorylation on Cdc28 is dependent on an intact *SWE1* and that tyrosine 19 is the target of phosphorylation. The level of tyrosine phosphorylation in the *elm1Δ* strain (Figure 2A, lane 3) was approximately twice that of in isogenic wild-type strain (Figure 2A, lane 2; see Materials and methods), suggesting that Swe1 kinase activity is increased in the absence of *ELM1*. Tyrosine phosphorylation on Cdc28 in the *elm1Δ* strain was dependent on *SWE1* and on tyrosine 19, as tyrosine phosphorylation was absent in the *elm1Δ swe1Δ* and *elm1Δ cdc28V18F19* strains (Figure 2A, lanes 5 and 7, respectively).

In order to quantitate the amount of Cdc28, which is tagged with the HA epitope, we stripped the original anti-phosphotyrosine Western blot and reprobed it with HA antibody (Figure 2B). The level of Cdc28 protein was essentially the same in every strain. This indicates that the difference in tyrosine phosphorylation reflected

either the difference in Swe1 kinase activity or the difference in Mih1 phosphatase activity in these strains.

Results similar to those shown in Figure 2 were obtained when phospho-cdc2 antibody, which specifically recognizes the phosphorylated Tyr15 residue of cdc2 protein (see Materials and methods), was used to probe the blots.

Together, our cell morphology studies and Cdc28 tyrosine phosphorylation analysis demonstrate that Elm1 may act as a negative regulator of Swe1 kinase activity and that Swe1 is responsible for the phosphorylation of the tyrosine 19 of Cdc28.

Figure 2. Cdc28 Y-19 phosphorylation is elevated in *elm1* mutants. Extracts were prepared from wild-type strain yWW336, *elm1* strain yWW411, *swe1* strain yWW665, *elm1 swe1* strain yWW669, *cdc28VF* strain yWW338, and *elm1 cdc28VF* strain yWW659. Cdc28-HA protein was immunoprecipitated from the extracts using 12CA5 HA antibody. The wild-type untagged strain yWW001 was included as a control for the specificity of immunoprecipitation. Cdc28-HA immunoprecipitates were resolved by SDS-PAGE, and the blot was probed with Cdc28 phosphotyrosine 19 antibody. The relative amount of tyrosine phosphoryaltion in each lane is indicated in arbitrary units below the upper panel. To normalize the amount of Cdc28 protein loaded in each lane, the western blot was stripped of phosphotyrosine antibody and reproved with 12CA5 HA antibody in the lower panel.

Figure 2

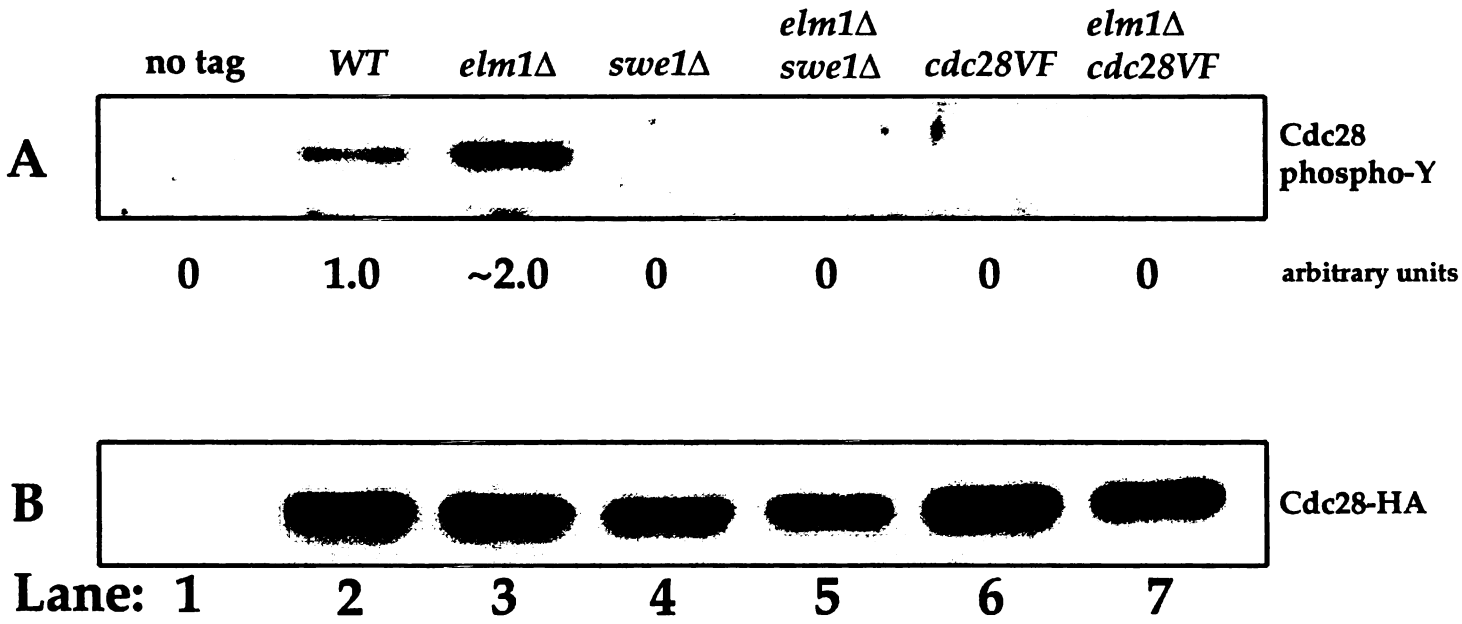
no tag
WT
elm1Δ
swe1Δ
elm1Δ swe1Δ
cdc28VF
elm1Δ cdc28VF
A
Cdc28 phospho-Y
0
1.0
~2.0
0
0
0
0
arbitrary units
B
Cdc28-HA
Lane: 1
2
3
4
5
6
7

ELM1 *regulates the level of Swe1 protein expression*

There are a couple of possible ways by which Elm1 might negatively regulate the level of Cdc28 Y-19 phosphorylation: Elm1 may affect the activity of Mih1 phosphatase or Elm1 may affect the activity of Swe1 kinase. We therefore examined the level of Swe1 protein in *elm1* mutants and in wild-type cells. In order to visualize Swe1 on Western blots, we have constructed a Swe1 fusion protein fused to tandem copies of the Myc epitope (see Materials and methods). We found that the *elm1Δ SWE1::myc13* cells exhibited elongated bud morphology similar to that of *elm1Δ SWE1* cells, suggesting that *SWE1::myc13* was functional; *SWE1::myc13* did not appear to be hyper-active, as the *SWE1::myc13* cells exhibited an ovoid cell shape similar to wild-type cells (data not shown).

In order to compare the expression level of Swe1-myc13 protein in various strains, whole-cell lysates were prepared (see Materials and methods). We observed that Swe1-myc13 was expressed in wild-type cells, as Myc antibody specifically identified a band of ~150 kd (Figure 3A, lane 2) which was absent from the no tag control strain (Figure 3A, lane 1). The level of Swe1-myc13 protein expression in *elm1Δ* cells was higher than that in wild-type cells (Figure 3A, lanes 2 and 3). Probing the same blot with antibody after stripping the Myc antibody (Figure 3B, lanes 2 and 3) demonstrated that equal amounts of protein were loaded in lanes 2 and 3.

To quantitate the relative amount of Swe1-myc13 in *elm1Δ* and wild-type cells, we loaded decreasing amounts of extracts from the

elm1Δ strain as follows: lane 3, 100%; lane 4, 67%; lane 5, 50%; and lane 6, 33%. We found that the intensity of the Swe1-myc13 signal in Figure 3A, lane 2 was between those of lane 4 and lane 5, i.e., *elm1Δ* cells accumulated Swe1-myc13 protein to a level 1.5- to 2.0-fold that of wild-type cells. We therefore conclude that Elm1 negatively regulates Swe1 kinase activity at least in part through down-regulation of Swe1 protein level.

Accumulation of the Swe1 protein in *elm1Δ* cells could be the result of two types of regulation: *ELM1* may affect *SWE1* mRNA expression; or *ELM1* may regulate the stability of Swe1 protein. We decided to study whether *ELM1* affects the transcription from the *SWE1* promoter. It has been shown that *SWE1* mRNA is predominantly transcribed in the S phase of the cell cycle (Ma et al., 1996) and increased Swe1 protein expression from the *GAL1* promoter leads to a G2 delay or arrest (Booher et al., 1993). To circumvent any effect of an altered cell cycle in *elm1Δ* cells that might have on the *SWE1* mRNA stability, we replaced the open reading frame of *SWE1* with that of *GFP* and followed instead the expression of the *GFP* mRNA. Yeast mRNA was isolated from wild-type, *swe1Δ::pSWE1::GFP*, and *elm1Δ swe1Δ::pSWE1::GFP* cells and separated on a Northern blot. Expression of *GFP* mRNA from the *SWE1* promoter was detected using a *GFP* probe and gel loading was controlled by probing the Northern blot with a *PFY1* probe. We found that expression of *GFP* mRNA was absent in the control strain and was at comparable levels in *ELM1* and in *elm1Δ* strains (data not shown). We therefore conclude that *ELM1* does not affect the promoter strength of *SWE1*.

Taken together, we conclude that *ELM1* regulates the level of Swe1 protein and this regulation does not occur at the *SWE1* promoter strength.

Figure 3. Swe1 protein level is higher in *elm1* mutants. Whole-cell lysates were prepared from control strain yWW018 (lane 1), *SWE1::myc*$_{13}$ strain yWW588 (lane 2), and *elm1 SWE1::myc*$_{13}$ strain yWW589 (lane 3). The blot was probed with Myc antibody. Decreasing amounts of samples from *elm1 SWE1::myc*$_{13}$ strain yWW589 were loaded in lane 3 (100%), lane 4 (67%), lane 5 (50%), and lane 6 (33%). To normalize the loading of protein samples, the Western blot was stripped of Myc antibody and re-probed with Ste12 antibody as shown in the lower panel.

Figure 3

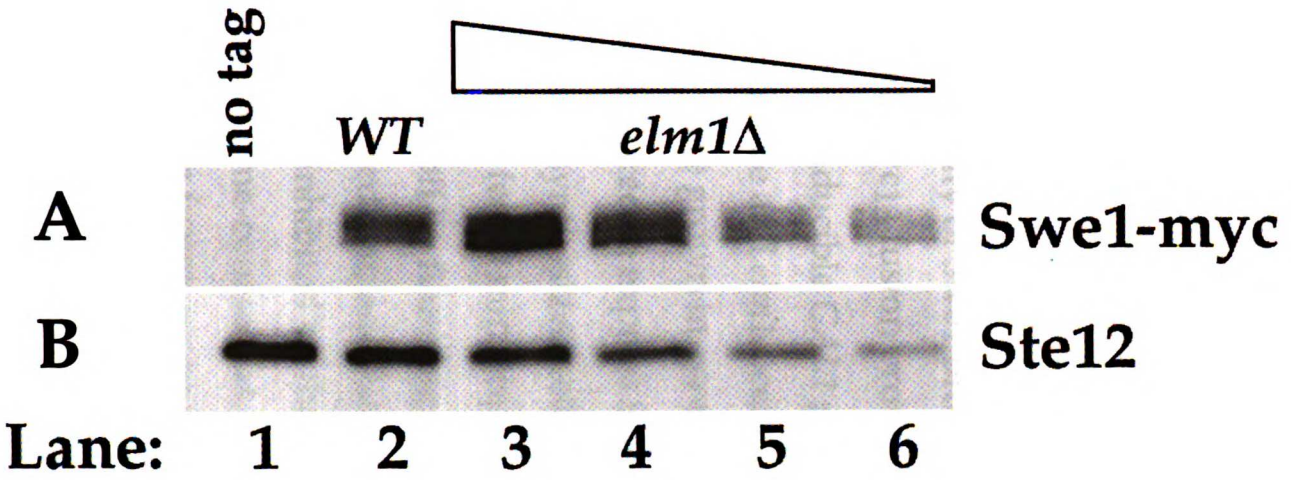

UCSF LIBRARY

Swe1 protein is stabilized in elm1 *mutants*

Since we observed that Swe1 protein accumulated to higher levels in *elm1* cells and that *SWE1* promoter strength was not affected in *elm1* mutants, we reasoned that the stability of Swe1 protein must be affected in *elm1* mutants.

To test this hypothesis we carried out pulse-chase labeling experiments to measure the stability of Swe1 protein in wild-type versus *elm1* strains. The Swe1-myc13 fusion protein was expressed under the control of a galactose inducible *GAL1* promoter (see Material and Methods). Wild-type and *elm1Δ* cells containing the P_{GAL1}*::SWE1::myc13* construct were grown in synthetic media omitted for methionine to log phase, induced to express Swe1-myc13 with galactose for 15 minutes. Newly synthesized cellular proteins were then labeled with [^{35}S]methionine for 10 minutes. *SWE1::myc13* mRNA expression was switched off by filtrating the culture and transferring the cells to glucose medium, and further labeling of newly synthesized proteins were inhibited by the addition of excess non-radioactive methionine. A time-course was followed at 0, 1, 2, and 3 hours of chase. Swe1-myc13 fusion protein was immunoprecipitated, separated on a SDS-PAGE gel, and exposed to a PhosphorImager storage screen (Figure 4A, upper panel). We observed that the rate of degradation of Swe1-myc13 protein was lower in *elm1* mutants than in wild-type cells.

In order to obtain a quantitative result, signals from the phosphorimager were quantitated using the ImageQuant software

and plotted in Figure 4B. The half-lives of Swe1-myc13 were deduced from the graph. We found the half-lives of Swe1-myc13 were 63 minutes in wild-type cells versus 129 minutes in *elm1* mutants in asynchronous grown cultures.

One caveat of the above half-life result is that the stability of Swe1-myc13 was measured in asynchronous yeast cultures. One conceivable possibility is that degradation of Swe1-myc13 is differentially regulated in various phases of the cell cycle and that *elm1* mutants accumulate at a cell cycle stage when degradation of Swe1 protein is slow. To eliminate this possibility, the pulse-chase labeling experiment was repeated with yeast cultures arrested in G2 with nocodazole for 2 hours prior to the addition of galactose and the nocodozole arrest was maintained throughout the experiment (Figure 4A, lower panel). We found that in this case the half-lives of Swe1-myc13 were 67 minutes in wild-type cells versus 244 minutes in *elm1* mutants (Figure 4B).

We conclude from our pulse-chase labeling experiments that *ELM1* affects the stability of Swe1 protein.

Figure 4. Stabilization of Swe1-myc$_{13}$ protein in *elm1* mutants. (A) P_{GAL1}*::SWE1::myc*$_{13}$ strain yWW648 and *elm1* P_{GAL1}*::SWE1::myc*$_{13}$ strain yWW684 were grown in raffinose medium and induced to express Swe1-myc$_{13}$ by addition of galactose for 15 minutes. Newly synthesized proteins were pulse labeled with [S-35]methionine for 10 minutes. Cells were harvested and resuspended in YEPD supplemented with 3mM non-radioactive methionine. Aliquots were taken at the indicated time-points. P_{GAL1}*::SWE1::myc*$_{13}$ strain grown in raffinose medium was labeled with [S-35]methionine for 10 minutes and served as a control. Experiments were carried out using asynchronous cultures and nocodazole arrested cultures. In the nocodazole arrest experiment, nocodazole was added to the media for 2 hours prior to the addition of galactose and was maintained throughout the experiment. ^{35}S-labeled Swe1-myc$_{13}$ was subject to immunoprecipitation. Proteins were separated by SDS-PAGE and the gels were exposed to a Phosphorimager screen. (B) The signals from the Phosphorimager screen were quantified using ImageQuant software. The values of half-lives of Swe1-myc$_{13}$ protein were deducted from the plots.

Figure 4A

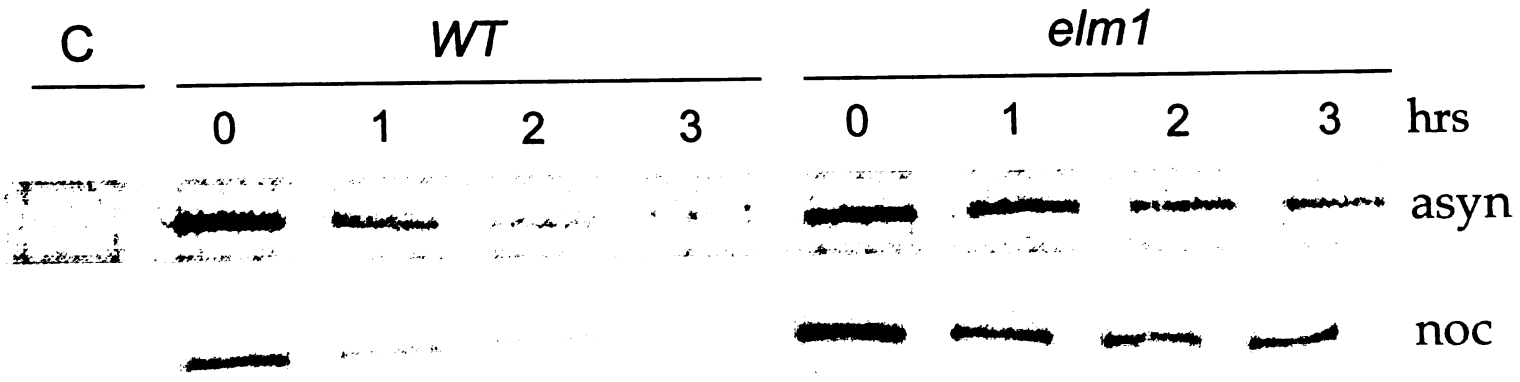

Figure 4B

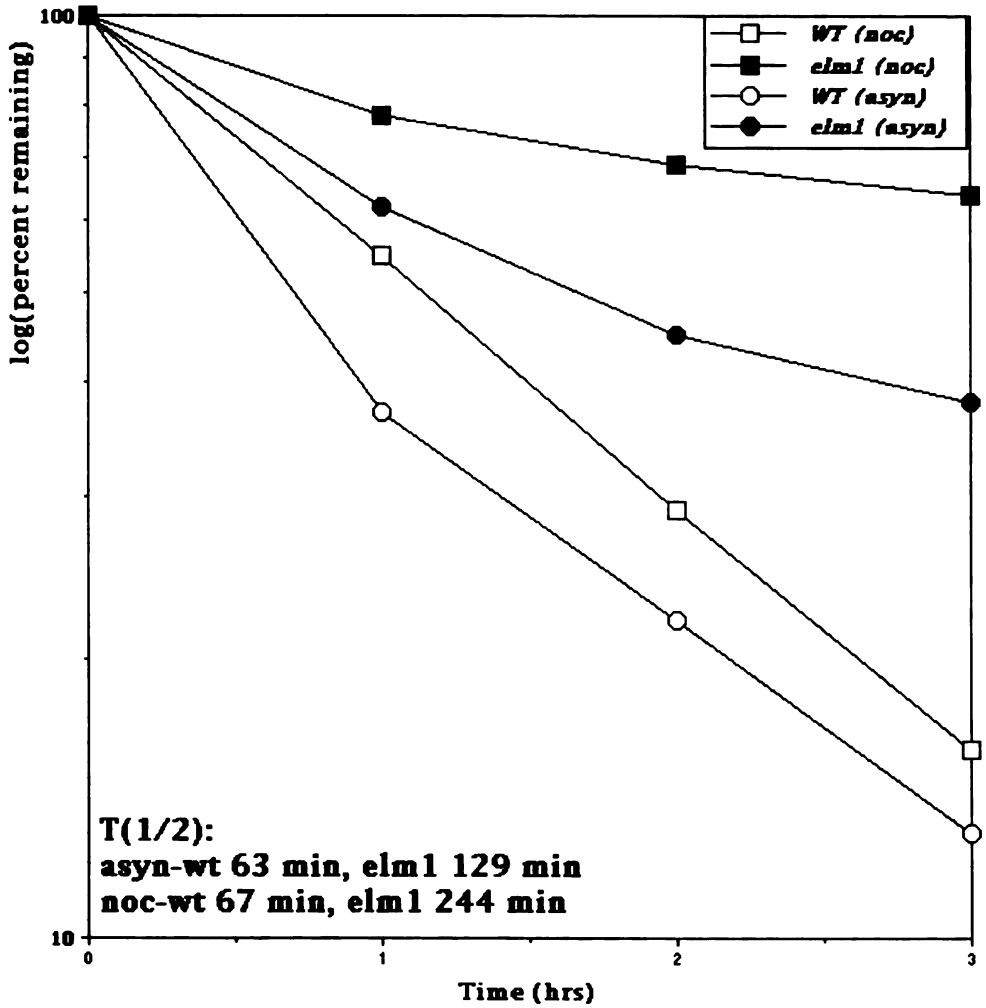
100
10
log(percent remaining)
WT (noc)
elm1 (noc)
WT (asyn)
elm1 (asyn)
T(1/2):
asyn-wt 63 min, elm1 129 min
noc-wt 67 min, elm1 244 min
0
1
2
3
Time (hrs)

Moderately elevated expression of Swe1 protein mimics elm1 *phenotype*

It has been observed that over-expression of Swe1 from a *GAL1* promoter results in highly elongated bud phenotype (Booher et al., 1993). Since we observed only moderate elevation of Swe1 protein level and moderate increase in Swe1 protein stability in *elm1* mutants, we asked whether moderately increasing the copy number of *SWE1* gene would be sufficient in mimicking *elm1* mutant phenotype. We generated an unmarked *swe1Δ::hisG* strain (see Material and Methods). We studied the cellular morphology of *swe1Δ::hisG pRS316, swe1Δ::hisG pRS316-SWE1, swe1Δ::hisG pRS313-SWE1 pRS314-SWE1 pRS315-SWE1 pRS316-SWE1,* and *elm1Δ swe1Δ::hisG pRS316-SWE1* strains (Figure 5A, panels *a, b, c,* and *d*). We found that cells from the *swe1Δ::hisG pRS316* strain exhibited similar wild-type oval bud morphology as that of *swe1Δ::hisG pRS316-SWE1.* However, about 10 percent of cells from the *swe1Δ::hisG pRS313-SWE1 pRS314-SWE1 pRS315-SWE1 pRS316-SWE1* strain exhibited an elongated bud phenotype. In comparison, about 40 percent of cells from the *elm1Δ swe1Δ::hisG pRS316-SWE1* strain exhibited an elongated bud phenotype.

In order to compare the level of Swe1 protein expression in aforementioned strains, we isolated whole-cell yeast lysates and separated proteins on a Western blot. A rabbit polyclonal Swe1 antibody was used to detect the expression of Swe1 protein (Figure 5B, upper panel). We observed that Swe1 protein was absent in *swe1Δ::hisG pRS316* strain (lane 1), demonstrating specificity of the Swe1 polyclonal antibody. We found that the level of Swe1 protein

was higher in *elm1Δ swe1Δ::hisG pRS316-SWE1* strain (lane 4) than in *swe1Δ::hisG pRS316-SWE1* strain (lane 2), while even higher amount of Swe1 protein was expressed in *swe1Δ::hisG pRS313-SWE1 pRS314-SWE1 pRS315-SWE1 pRS316-SWE1* cells (lane 3). Probing the same blot with Ste12 antibody after stripping the Swe1 antibody demonstrated that equal amounts of proteins were loaded in each lane (Figure 5B, lower panel).

We conclude that moderate elevation of Swe1 protein expression in budding yeast is sufficient in inducing elongated bud phenotype.

Figure 5. Moderately elevated expression of Swe1 is sufficient in inducing elongated bud morphology in budding yeast. A) A *swe1* deletion strain carrying a) the cen-ars vector pRS316, yWW951; b) the cen-ars pRS316-Swe1 plasmid, yWW952; c) plasmids pRS313-Swe1 pRS314-Swe1 pRS315-Swe1 pRS316-Swe1, yWW953; and d) *elm1 swe1* strain carrying the cen-ars pRS316-Swe1 plasmid, yWW954 were grown in synthetic glucose growth media with appropriate omissions of nucleotides and amino acids to exponential growth phase. Cellular morphologies were examined using Nomarski optics. B) In order to compare the Swe1 protein expression levels in various strains, total cell lysates were prepared from strains yWW951, yWW952, yWW953, and yWW954. Proteins were resolved using SDS-PAGE and the Western blot was probed with a rabbit Swe1 polyclonal antibody.

Figure 5A

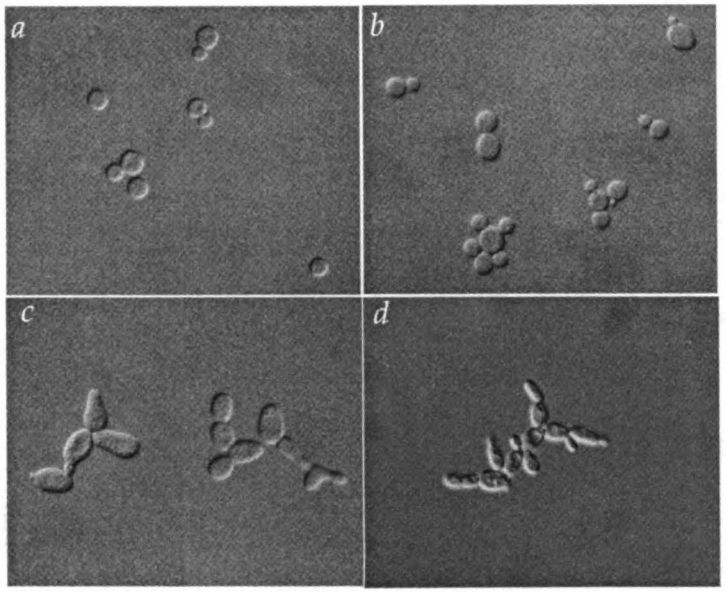

Figure 5B

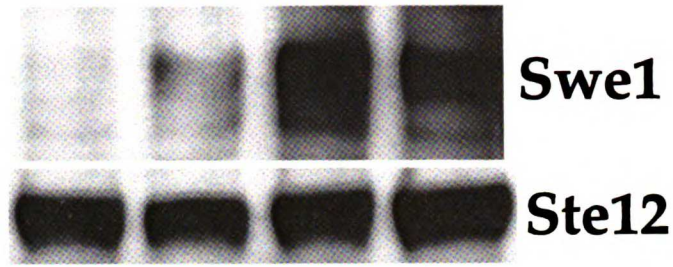

Lane: 1 2 3 4

UCSF LIBRARY

Cdc28 Tyrosine 19 phosphorylation peaks in the G2 phase of the cell cycle

We were puzzled by the observation that even though Swe1 protein expression in *swe1Δ::hisG pRS313-SWE1 pRS314-SWE1 pRS315-SWE1 pRS316-SWE1* strain was higher than that in *elm1Δ swe1Δ::hisG pRS316-SWE1* strain, the percentage of cells exhibiting an elongated bud morphology was lower. This observation implied that the level of Swe1 protein expression alone might not be solely reflective of *SWE1* activity. We therefore carried out a cell-cycle synchrony study of Swe1 protein expression and its kinase activity. A yeast strain *MATa SWE1::myc13 CDC28::HA CLN2::HA* was generated from the diploid strain yWW703. Cells were treated with alpha-mating factor for 90 minutes to arrest them in the G1 phase of the cell cycle. At the release time-point, alpha-mating factor was washed away and the cells were resuspended in fresh medium. Aliquots of the culture were taken every 15 minutes. Whole-cell lysates were prepared from the aliquots and proteins were separated on a Western blot. A protein sample from an asynchronous grown culture of *MATa SWE1::myc13 CDC28::HA CLN2::HA* was included as control. Myc antibody was used to probe the high molecular weight portion of the blot to detect the expression of Swe1-myc13 protein and Cdc28 phosphotyrosine 19 antibody was used to probe the low molecular weight portion of the blot (Figure 6A).

We found that Swe1-myc13 protein expression was absent in alpha-mating factor arrested cells at 0 minutes. Swe1-myc13 protein first appeared at 45 minutes, peaked at 60 minutes, and trailed off at

75 minutes after the mating-factor release. Its expression level increased again around 105 minutes during apparently the second cell cycle.

To our surprise, Cdc28 tyrosine 19 phosphorylation first appeared at 60 minutes and peaked at 75 minutes after the mating-factor release when Swe1 protein level was apparently low. Cdc28 tyrosine 19 phosphorylation was absent from 90 to 105 minutes after release.

In order to control the cell cycle synchrony and the loading of the gel, the blots were stripped of antibodies and re-probed with the HA antibody. Probing the blots with the HA antibody to detect Cdc28-HA demonstrated that the lanes were evenly loaded and probing the blot with the HA antibody to detect the Cln2-HA demonstrated that cells were synchronized in progressing through the cell cycle.

We also examined bud size of cells from the culture aliquots in order to visually monitor the synchrony of the release and to follow the progression of the cell cycle. We found that small buds first emerged at 45 minutes, indicating that the cells were in the G1/S phase transition. The cells were large budded at 75 minutes, indicating that the cells were in G2 phase. At 90 minutes, most cells had divided and at 105 minutes small buds appeared indicating they have progressed to the next G1/S phase transition (data not shown).

In order to understand the regulation of *ELM1* on Swe1 kinase activity, we generated a yeast strain *MATa elm1 SWE1::myc13 CDC28::HA CLN2::HA* from the diploid yWW703 and carried out identical alpha mating-factor cell cycle arrest and release experiments (Figure 6B). Despite the abnormal bud morphology of *elm1* mutant

cells, they responded similarly to alpha mating-factor treatment as wild-type cells by generating shmoos to over 90 percent of the cell population after 90 minutes of treatment. We found that in the *elm1* background Swe1-myc13 protein first appeared at 45 minutes and peaked at 60 minutes after the release (Figure 6B), which was similar to that in wild-type background (Figure 6A). However, Swe1-myc13 protein was still present at 75 minutes after the release. Cdc28 tyrosine 19 phosphorylation first appeared at 60 minutes and peaked at 75 minutes, which is similar to that in wild-type background. However, tyrosine 19 phosphorylation lingered till 90 minutes after release.

We conclude from our cell-cycle synchrony study that while Swe1 protein expression peaks earlier in the S phase of the cell cycle, its kinase activity peaks in the G2 phase of the cell cycle. We also conclude that *ELM1* regulates both the cell cycle expression pattern of Swe1 protein and that of its kinase activity.

Figure 6. Cell cycle regulation of Cdc28 tyrosine 19 phosphorylation in wild-type and in *elm1* mutants. A) Cells of *MATa SWE1::myc*$_{13}$ *CLN2::HA CDC28::HA* strain grown in YEPD medium were treated with alpha mating factor for 90 minutes and released from the G1 arrest by washing away the mating factor and resuspending in fresh growth medium. Aliquots of the culture were taken at specified time-points after release. A sample was also taken from a culture that was not treated with mating factor to use as a control. Proteins were resolved using SDS-PAGE. Myc antibody was used to probe the high molecular weight portion of the blot and Cdc28 phosphotyrosine 19 antibody was used to probe the low molecular weight portion of the blot. The blots were stripped of antibodies and re-probed with HA antibody to detect Cln2-HA and Cdc28-HA respectively. B) Identical experiments to that shown in A) were carried out using cells of *MATa elm1 SWE1::myc*$_{13}$ *CLN2::HA CDC28::HA* strain.

Figure 6a

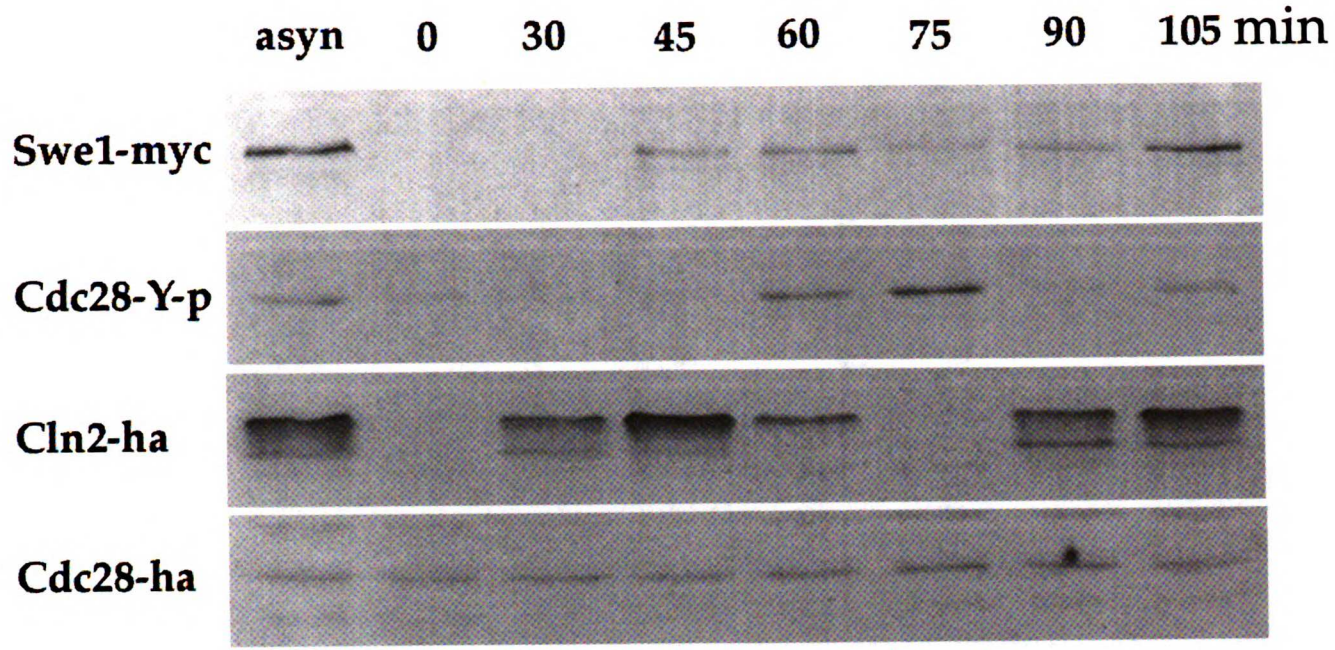

@f arrest and release

Figure 6b

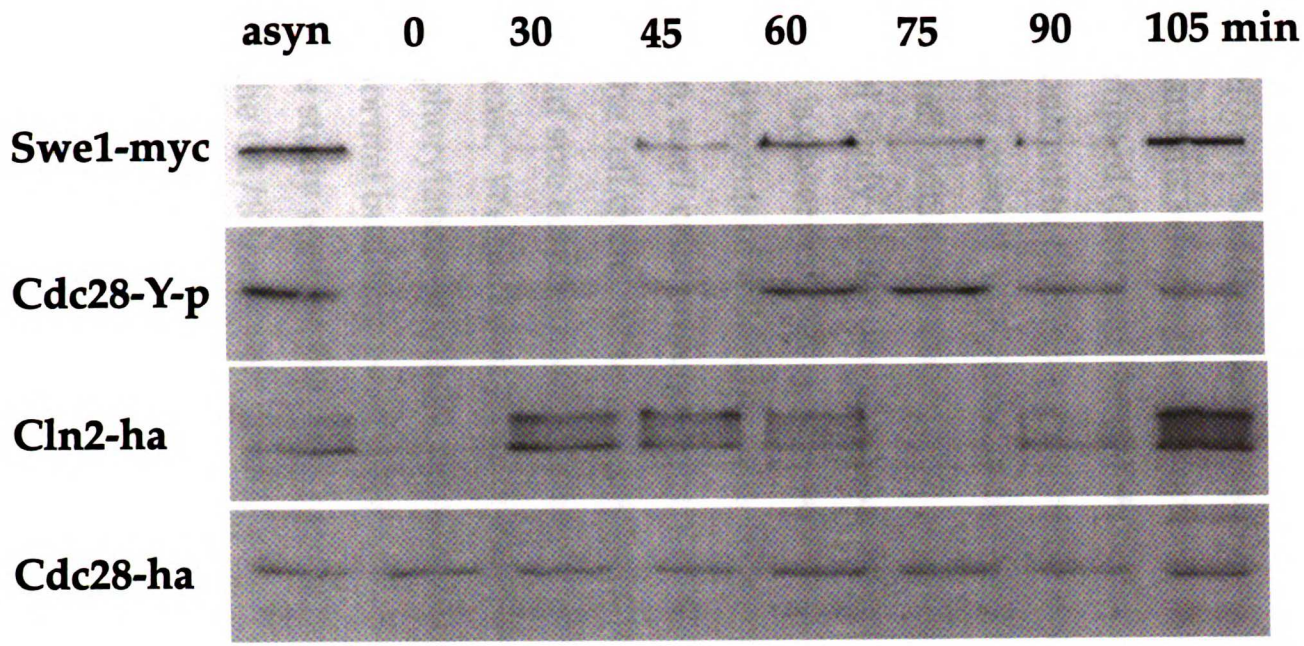

@f arrest and release

UCSF LIBRARY

Discussion

Function of Swe1 and Cdc28 Y-19 phosphorylation in budding yeast

SWE1 function in budding yeast is apparently important in checkpoint mechanisms when either the actin cytoskeleton or the septin ring is disrupted (Lew and Reed, 1995a; Sia et al., 1996; Barral et al., 1999). In contrast to the finding in fission yeast that wee1 is involved in cell size control, mutations in the *SWE1* gene in budding yeast did not initially yield any observable phenotype (Booher et al., 1993). In a careful study of the daughter cell volume of *swe1* and wild-type cells, it is observed that newly born *swe1* daughter cells are smaller compared to that of wild-type cells (Harvey and Kellogg, 2003). In addition, *swe1* cells undergo compensatory growth during the G1 phase of the cell cycle. Thus it is argued that Swe1 functions in a conserved bud size control mechanism in mitosis like that by wee1 in fission yeast. We find that there is basal Swe1-dependent tyrosine 19 phosphorylation of Cdc28, demonstrating that Swe1 is active during a normal budding yeast cell cycle. In a mating factor arrest and release study we find that Swe1 protein expression first appears during the G1/S transition, peaks in S phase, and trails off in the G2 phase of the cell cycle. Swe1 kinase activity, i.e., the level of Cdc28 Y-19 phosphorylation, however peaks surprisingly later in the G2 phase of the cell cycle when most of the Swe1 protein is absent. This observation is consistent with the finding that Swe1 is a specific inhibitory kinase towards Cdc28 complexed with a G2 cyclin, Clb2, but not towards Cdc28 complexed with a G1 cyclin, Cln2 (Booher et

al., 1993). This observation also suggests that the low level of Swe1 protein present in the G2 phase of the cell cycle is highly active and contributes to the majority of Y-19 phosphorylation on Cdc28. Our results support a role for Swe1 in a normal budding yeast cell cycle and suggest that the main function of Swe1 and Y-19 phosphorylation on Cdc28 is to prevent premature activation of the Cdc28-Clb2 complex. A safeguard mechanism against premature activation of the Cdc28-Clb2 complex may be important not only because it allows buds to reach critical volume before mitosis but also because Cdc28-Clb2 activity interferes with the formation of pre-replicative complex (Detweiler and Li, 1998).

Regulation of Swe1 degradation by Elm1

ELM1 has been identified in our screen for mutants that are defective in the switch from polar to isotropic bud growth. *ELM1* is found to be a negative regulator of *SWE1* function, since a mutation in the *SWE1* gene suppressed the elongated bud phenotype and G2 delay of *elm1* mutants (Edgington et al., 1999; Sreenivasan and Kellogg, 1999). We find that *elm1* mutant cells contain higher levels of Swe1 protein. We also demonstrate that Elm1 negatively regulates Swe1 at the post-transcriptional level, i.e., Elm1 negatively regulates the protein stability of Swe1. The difference in Swe1 protein stability in wild-type cells and in *elm1* cells is more pronounced when the protein half-life measurements are carried out in cells arrested in G2. The larger difference in Swe1 protein half-life may reflect physiological relevance, as G2 is the cell cycle phase in which Swe1 is

most active and also when most of the Swe1 protein is turned over. Our mating factor arrest and release experiments demonstrate that Cdc28 tyrosine 19 phosphorylation in *elm1* mutants is extended for at least 15 minutes longer in G2 when compared to that in wild-type cells. *ELM1* therefore is required for the timely down-regulation of Swe1 kinase activity in the G2 phase of the cell cycle.

Currently the protein machinery involved in the degradation of Swe1 in budding yeast is not well understood. It has been reported that the SCF-Met30 E3 ubiquitin ligase acting in conjunction with the E2 ubiquitin-conjugating enzyme Cdc34 are involved in the degradation of Swe1 (Kaiser et al., 1998). However, it has been observed that at least under certain circumstances, Met30 is not involved in the degradation of Swe1 (McMillan et al., 2002). In fission yeast Tome-1 associates with Skp1 and affects the degradation of wee1, thus appears to act as an E3 ubiquitin ligase (Ayad et al., 2003). No sequence homolog of Tome-1 is present in budding yeast.

It has been observed that Swe1 itself is a phospho-protein and the phosphorylation on Swe1 is reduced in *elm1* mutants *in vivo* (Sreenivasan and Kellogg, 1999). We have observed that yeast lysates prepared from *elm1* mutants exhibit reduced phosphorylation on Swe1 in an *in vitro* study (data not shown) compared to yeast lysates prepared from wild-type cells. Currently there is no direct evidence to indicate that Swe1 is a substrate of Elm1 kinase, and it is not known whether phosphorylation of Swe1 is required for its degradation. Cdc28-Clb2 kinase itself has been shown to be able to phosphorylate Swe1 (McMillan et al., 2002). It is yet to be established whether Cdc28 phosphorylation of Swe1 plays any role in Swe1 degradation.

Elm1 has been shown to localize to the yeast bud neck (Moriya and Isono, 1999; Bouquin et al., 2000; Thomas et al., 2003; our unpublished results). It is found that localization of Elm1 to the bud neck is dependent on the integrity of the septin ring (Bouquin et al., 2000; Thomas et. al., 2003; our unpublished results). Elm1 therefore apparently acts in the same bud morphogenesis checkpoint that involves the septins, nim1 homologues, and Swe1 (Barral et al., 1999). Interestingly Swe1 is localized to both the nucleus and the bud neck. Localization of Swe1 to the bud neck is dependent on the function of its interacting protein Hsl7 (Shulewitz et al., 1999; Longtine et al., 2000; Cid et al., 2001). It is therefore plausible that the negative regulation of Swe1 by the cohorts of Elm1 and nim1 homologues is spatially restricted at the bud neck.

References

Ahn, S.H., A. Acurio, and S.J. Kron. 1999. Regulation of G2/M progression by the STE mitogen-activated protein kinase pathway in budding yeast filamentous growth. *Mol. Biol. Cell* **10**: 3301-16.

Ahn, S.H., B.T. Tobe, J.N. Fitz Gerald, S.L. Anderson, A. Acurio, and S.J. Kron. 2001. Enhanced cell polarity in mutants of the budding yeast cyclin-dependent kinase Cdc28p. *Mol. Biol. Cell* **12**: 3589-600.

Altman, R. and D. Kellogg. 1997. Control of mitotic events by Nap1 and the Gin4 kinase. *J. Cell Biol.* **138**: 119-130.

Amon, A., U. Surana, I. Muroff, and K. Nasmyth. 1992. Regulation of $p34^{CDC28}$ tyrosine phosphorylation is not required for entry into mitosis in *S. cerevisiae. Nature* **355:** 368-371.

Ayad, N.G., S. Rankin, M. Murakami, J. Jebanathirajah, S. Gygi, and M.W. Kirschner. 2003. Tome-1, a trigger of mitotic entry, is degraded during G1 via the APC. *Cell* **113:** 101-13.

Barral, Y., M. Parra, S. Bidlingmaier, and M. Snyder. 1999. Nim1-related kinases coordinate cell cycle progression with the organization of the peripheral cytoskeleton in yeast. *Genes & Dev.* **13**: 176-187.

Blacketer, M.J., C.M. Koehler, S.G. Coats, A.M. Myers, and P. Madaule. 1993. Regulation of dimorphism in *Saccharomyces cerevisiae*: involvement of the novel protein kinase homolog Elm1p and protein phosphatase 2A. *Mol. Cell. Biol.* **13**: 5567-5581.

Blacketer M.J., P. Madaule, and A.M. Myers. 1995. Mutational analysis of morphologic differentiation in *Saccharomyces cerevisiae*. *Genetics* **140**: 1259-1275.

Booher, R.N., R.J. Deshaies, and M.W. Kirschner. 1993. Properties of *Saccharomyces cerevisiae* wee1 and its differential regulation of $p34^{CDC28}$ in response to G1 and G2 cyclins. *EMBO J.* **12**: 3417-3426.

Bouquin, N., Y. Barral, R. Courbyrette, M. Blondel, M, Snyder, and C. Mann. 2000. Regulation of cytokinesis by the Elm1 protein kinase in *Saccharomyces cerevisiae*. *J. Cell Sci.* **113**: 1435-1445.

Cid, V.J., M.J. Shulewitz, K.L. McDonald, and J. Thorner. 2001. Dynamic localization of the Swe1 regulator Hsl7 during the *Saccharomyces cerevisiae* cell cycle. *Mol. Biol. Cell* **12**: 1645-69.

Cross, F.R. 1988. *DAF1*, a mutant gene affecting size control, pheromone arrest, and cell cycle kinetics of *Saccharomyces cerevisiae*. *Mol. Cell. Biol.* **8**: 4675-84.

Detweiler, C.S., J.J. Li. 1998. Ectopic induction of Clb2 in early G1 phase is sufficient to block prereplicative complex formation in Saccharomyces cerevisiae. *Proc. Natl. Acad. Sci.* **95:** 2384-9.

Enoch, T. and P. Nurse. 1990. Mutation of fission yeast cell cycle control genes abolishes dependence of mitosis on DNA replication. *Cell* **60**: 665-673.

Edgington, N. P., M. J. Blacketer, T. A. Bierwagen, and A. M. Myers. 1999. Control of *Saccharomyces cerevisiae* filamentous growth by cyclin-dependent kinase Cdc28. *Mol. Cell. Biol.* **19**: 1369-1380.

Guthrie, C. and G.R. Fink. 1991. Guide to yeast genetics and molecular biology. *Meth. Enzymol.* **194**: 1-933.

Harlow, E. and D. Lane. 1989. Antibodies: A laboratory manual. 2nd ed. Cold Spring Harbor Laboratory Press, Cold Spring Harbor, NY.

Harvey, S.L. and D.R. Kellogg. 2003. Conservation of mechanisms controlling entry into mitosis: Budding yeast wee1 delays entry into mitosis and is required for cell size control. *Curr. Biol.* **13:** 264-275.

Kaiser, P., R.A.L. Sia, E.G.S. Bardes, D.J. Lew, and S.I. Reed. 1998. Cdc34 and the F-box protein Met30 are required for degradation of the Cdk-inhibitory kinase Swe1. *Genes Dev.* **12:** 2587–2597.

Kellogg, D.R. and A.W. Murray. 1995. Nap1 acts with Clb2 to perform mitotic functions and to suppress polar bud growth in budding yeast. *J. Cell Biol.* **130**: 675-685.

Koehler, C.M. and A.M. Myers. 1997. Serine-threonine protein kinase activity of Elm1p, a regulator of morphologic differentiation in *Saccharomyces cerevisiae*. *FEBS Letters* **408**: 109-114.

Lew, D.J. and S.I. Reed. 1993. Morphogenesis in the yeast cell cycle: Regulation by Cdc28 and cyclins. *J. Cell Biol.* **120**: 1305-1320.

Lew, D.J. and S.I. Reed. 1995a. A cell cycle checkpoint monitors cell morphogenesis in budding yeast. *J. Cell Biol.* **129**: 739-749.

Lew, D.J. and S.I. Reed. 1995b. Cell cycle control of morphogenesis in budding yeast. *Curr. Opin. Genet. Dev.* **5**: 17-23.

Lim, H.H., P.Y. Goh, and U. Surana. 1996. Spindle pole body separation in *Saccharomyces cerevisiae* requires dephosphorylation of the tyrosine 19 residue of Cdc28. *Mol. Cell. Biol.* **16**: 6385-6397.

Longtine, M.S., A. McKenzie, D.J. Demarini, N.G. Shah, A. Wach, A. Brachat, P. Philippsen, and J.R. Pringle. 1998a. Additional modules for versatile and economical PCR-based gene deletion and modification in *Saccharomyces cerevisiae*. *Yeast* **14**: 953-961.

Longtine, M.S., H. Fares, and J.R. Pringle. 1998b. Role of the yeast Gin4p and the relationship between septin assembly and septin function. *J. Cell Biol.* **143**: 719-736.

Longtine, M.S., C.L. Theesfeld, J.N. McMillan, E. Weaver, J.R. Pringle, and D.J. Lew. 2000. Septin-dependent assembly of a cell cycle-

regulatory module in *Saccharomyces cerevisiae. Mol. Cell. Biol.* **20**: 4049-61.

Ma, X.-J., Q. Lu, and M. Grunstein. 1996. A search for proteins that interact genetically with histone H3 and H4 amino termini uncovers novel regulators of the Swe1 kinase in *Saccharomyces cerevisiae. Genes & Dev.* **10**: 1327-1340.

McMillan J.N., C.L. Theesfeld, J.C. Harrison, E.S. Bardes, and D.J. Lew. 2002. Determinants of Swe1p Degradation in *Saccharomyces cerevisiae. Mol. Biol. Cell* **13:** 3560-3575.

Moriya, H. and K. Isono. 1999. Analysis of genetic interactions between *DHH1, SSD1* and *ELM1* indicates their involvement in cellular morphology determination in *Saccharomyces cerevisiae. Yeast* **15**: 481-96.

Parker, L.L., S.A. Walter, P.G. Young, and H. Piwnica-Worms. 1993. Phosphorylation and inactivation of the mitotic inhibitor wee1 by the nim1/cdr1 kinase. *Nature* **363**: 736-738.

Parker, L.L., P.J. Sylvestre, M.J. Byrnes, F. Liu, and H. Piwnica-Worms. 1995. Identification of a 95-kDa WEE1-like tyrosine kinase in HeLa cells. *Proc. Natl. Acad. Sci.* **92**: 9638-9642.

Rhind, N., B. Furnari, and P. Russell. 1997. Cdc2 tyrosine phosphorylation is required for the DNA damage checkpoint in fission yeast. *Genes & Dev.* **11**: 504-511.

Russell, P. and P. Nurse. 1987a. Negative regulation of mitosis by Wee1, a gene encoding a protein kinase homolog. *Cell* **49**: 559-567.

Russell, P. and P. Nurse. 1987b. The mitotic inducer nim1 functions in a regulatory network of protein kinase homologs controlling the initiation of mitosis. *Cell* **49**: 569-576.

Russell, P., S. Moreno, and S.I. Reed. 1989. Conservation of mitotic controls in fission and budding yeasts. *Cell* **57:** 295-303.

Sambrook, J., E.F. Fritsch, and T. Maniatis. 1989. Molecular Cloning: A Laboratory Manual. 2nd ed. Cold Spring Harbor Laboratory Press, Cold Spring Harbor, NY.

Shulewitz, M.J., C.J. Inouye, and J. Thorner. 1999. Hsl7 localizes to a septin ring and serves as an adapter in a regulatory pathway that relieves tyrosine phosphorylation of Cdc28 protein kinase in *Saccharomyces cerevisiae*. *Mol. Cell. Biol.* **19**: 7123-37.

Sia, R.A., H.A. Herald, and D.J. Lew. 1996. Cdc28 tyrosine phosphorylation and the morphogenesis checkpoint in budding yeast. *Mol. Biol. Cell* **7:** 1657-1666.

Sikorski, R.S. and P. Hieter. 1989. A system of shuttle vectors and yeast host strains designed for efficient manipulation of DNA *in Saccharomyces cerevisiae*. *Genetics* **122**: 19-27.

Sorger, P.K. and A.W. Murray. 1992. S-phase feedback control in budding yeast independent of tyrosine phosphorylation of p34*CDC28*. *Nature* **355**: 365-368.

Sreenivasan, A., and D. Kellogg. 1999. The Elm1 kinase functions in a mitotic signaling network in budding yeast. *Mol. Cell. Biol.* **19:** 7983–7994.

Thomas, C.L., M.J. Blacketer, N.P. Edgington, and A.M. Myers. 2003. Assembly interdependence among the *S. cerevisiae* bud neck ring proteins Elm1p, Hsl1p and Cdc12p. *Yeast* **20**: 813-26.

Wu, L. and P. Russell. 1993. Nim1 kinase promotes mitosis by inactivating wee1 tyrosine kinase. *Nature* **363**: 738-741.

Chapter 3.

Function of Elm1 in the bud morphogenesis checkpoint pathway

Abstract

Elm1 is a protein kinase that regulates budding yeast morphogenesis through down-regulation of the Swe1 kinase activity. To better understand Elm1 function we have studied the cellular localization of Elm1 protein. We find that Elm1 is localized specifically to the bud neck and this localization is dependent on the septin ring integrity. We find that the C-terminal domain of Elm1 is necessary and sufficient for its localization to the bud neck. We find that like *elm1* mutants, septin mutants contain elevated levels of Swe1-dependent Cdc28 tyrosine 19 phosphorylation. We argue that Elm1 is involved in a bud morphogenesis checkpoint pathway that monitors the septin ring integrity.

Introduction

In order to undergo one round of successful cell division, a budding yeast cell must coordinate accurately multiple critical events both temporally and spatially. Checkpoint mechanisms exist in budding yeast that monitor the completion of DNA replication, DNA damage, and mitotic spindle assembly (Enoch and Nurse, 1990; Rhind et al., 1997; Li and Murray, 1991). These checkpoint mechanisms prevent aberrant progression of the cell cycle before critical events are accomplished or damage is repaired. Yeast cells divide by generation of a new bud and its subsequent enlargement to a critical size before mitotic division. Morphogenesis checkpoint mechanisms in budding yeast that monitor the actin cytoskeleton assembly and the septin ring integrity have been described (Lew et al., 1995; Barral et al., 1999). Cyclin-dependent kinase, Cdc28, apparently is the target of the morphogenesis checkpoints, as both actin cytoskeleton disruption and the septin ring defect result in a Swe1-dependent G2 delay.

Septins are a family of GTP-binding proteins that were first identified in a screen for temperature sensitive mutants defective in cell cycle progression (Hartwell, 1971; Hartwell, 1973). Mutations in the septin genes lead to formation of elongated buds with multiple nuclei; cells remain attached due to a defect in cytokinesis. Members of the septin family of proteins, Cdc3, Cdc10, Cdc11, Cdc12, and Sep7, form into a ring of 10-nm filaments at the bud neck that is associated with the plasma membrane (Byers and Goetsch, 1976; Ford and Pringle, 1991; Kim et al., 1991; Frazier et al., 1998). Localization

of a large number of proteins to the bud neck requires the function of the septins. In particular, the nim1 homologues in budding yeast are localized to the bud neck in a septin-dependent manner (Okuzaki et al., 1997; Longtine et al., 1998; Barral et al., 1999). Mutations affecting the *S. cerevisiae* nim1 homologues also confer an elongated-bud phenotype (Ma et al., 1996; Altman and Kellogg, 1997; Longtine et al., 1998; Barrall et al., 1999). It has been observed that the morphological phenotypes of mutants defective in septins or in the nim1 homologues are reversed by mutations in *SWE1* (Ma et al., 1996; Longtine et al., 1998; Barral et al., 1999). Interestingly, Swe1 itself has been demonstrated to localize to both the nucleus and the bud neck (Longtine et al., 2000). Localization of Swe1 to the bud neck is dependent on Hsl1 and the septins. These findings suggest that Swe1 functions in the apical to isotropic switch and that septins and the nim1 homologues may control Swe1 activity at the bud neck.

Many proteins function at specific locations of the cell. In order to better understand Elm1 function in budding yeast, we have examined the cellular localization of the Elm1 protein. We find that Elm1 is localized to the bud neck. We demonstrate that Elm1 protein C-terminal domain is both necessary and sufficient for its bud-neck localization. We observe that localization of Elm1 to the bud neck is dependent on the septin ring integrity. We find that like in *elm1* mutants, septin mutants contain elevated level of Swe1-dependent Cdc28 tyrosine 19 phosphorylation. We argue that Elm1 is involved in a morphogenesis checkpoint mechanism that monitors the septin ring integrity.

Materials and methods

DNA manipulations, yeast strains, and media

Yeast strains used in this study are listed in Table 1. Yeast growth media and genetic manipulations were as described (Guthrie and Fink, 1991). DNA manipulations are as described in Sambrook et al. (1989).

Plasmid constructions

ELM1 deletion. A 3.4 kb XbaI fragment of the genomic sequence containing the *ELM1* gene was cloned in plasmid pRS306 (Sikorski and Hieter, 1989). The plasmid was cut with HpaI, releasing most of the *ELM1* ORF. The 6.0 kb fragment containing the pRS306 backbone and the 5′ and 3′ flanking region of the *ELM1* ORF was ligated to a 1.1 kb *TRP1* fragment, resulting in a plasmid in which the *ELM1* ORF was replaced by *TRP1*. The resulting *elm1Δ::TRP1* plasmid was cut with ClaI to target the disruption of the *ELM1* gene in the yeast genome.

Table 1. Strains used in this study.

Strain	Relevant genotype	Origin
yWW001	*MATa ade2 his3 leu2 trp1 ura3 can1 psi+ GAL+*	IH collection[a]
yWW018	*MATα ade2 his3 leu2 trp1 ura3 can1 psi+ GAL+*	IH collection[a]
yWW274	*MATa elm1::TRP1*	this study[a]
yWW305	*MATa swe1::LEU2*	this study[a]
yWW447	*MATa elm1::TRP1 swe1::LEU2*	this study[a]
yWW489	*MATα swe1::P_{GAL1}::SWE1-HA_2::LEU2*	this study[a]
yWW576	*MATa cdc12-6 ura3 leu2*	Pringle collection
yWW577	*MATa cdc12-6 leu2::pRS305-CDC12*	this study[b]
yWW584	*MATa cdc12-6 swe::LEU2*	this study[b]
yWW336	*MATa CDC28-HA::URA3*	Rudner and Murray[a]
yWW515	*MATa pRS316-ELM1-GFP elm1::TRP1*	this study[a]
yWW582	*MATa pRS316-ELM1-GFP cdc28-13 elm1::TRP1*	this study[a]
yWW520	*MATa pRS316-ELM1-GFP cdc28-1N*	this study[a]
yWW525	*MATa cdc12-6 pRS316-ELM1-GFP*	this study[b]
yWW583	*MATa cdc12-6 pRS316-ELM1-GFP leu2::PRS305-CDC12*	this study[b]
yWW585	*MATa cdc12-6 CDC28-HA::URA3*	this study[c]
yWW586	*MATa cdc12-6 CDC28-HA::URA3 leu2::pRS305-CDC12*	this study[d]
yWW587	*MATa cdc12-6 CDC28-HA::URA3 swe1::LEU2*	this study[d]
yWW617	*MATα leu2::pRS305-P_{ELM1}-GFP*	this study[a]
yWW618	*MATα leu2::pRS305-P_{ELM1}-GFP-ELM1(1-420)*	this study[a]
yWW619	*MATα leu2::pRS305-P_{ELM1}-GFP-ELM1(420-640)*	this study[a]
yWW620	*MATα leu2::pRS305-P_{ELM1}-GFP-ELM1(1-640)*	this study[a]
yWW627	*MATa elm1::TRP1 leu2::pRS305-P_{ELM1}-GFP*	this study[a]
yWW628	*MATa elm1::TRP1 leu2::pRS305-P_{ELM1}-GFP-ELM1(1-420)*	this study[a]
yWW629	*MATa elm1::TRP1 leu2::pRS305-P_{ELM1}-GFP-ELM1(420-640)*	this study[a]
yWW630	*MATa elm1::TRP1 leu2::pRS305-P_{ELM1}-GFP-ELM1(1-640)*	this study[a]

a. Strains are in the W303 background.

b. Strains are derived from yWW576.

c. Derived from the cross between yWW018 and yWW576.

d. Strains are derived from yWW585.

pRS316-ELM1::GFP. A BamHI site was introduced just before the stop codon of *ELM1* by a three-part ligation reaction. Fragment 1: a plasmid containing the *ELM1* gene was used as template for PCR amplification using primers 5′-AGTCAATTGCCGCGGCATTAATAC-3′ and 5′-CCTGTAGTTTCATCTAGGATCCACCATTATCTGCAAAG -3′. The PCR product was digested with SacII and BamHI at the sites underlined. Fragment 2: the PCR product using the *ELM1* plasmid as template and primers 5′-CTTTGCAGATAATGGTGGATCCTAGATGAAACTACAGG-3′ and 5′-CTTCATGGAATTGTCGACAGAAGGACT-3′ was digested with BamHI and SalI at the sites underlined. Fragment 3: the plasmid pRS316 (Sikorski and Hieter, 1989) was digested with SacII and SalI. A ligation reaction was carried out using the three digested DNA fragments, yielding plasmid pRS316-ELM1(BamHI). This plasmid was cut with BamHI and ligated to a GFP BamHI fragment (kindly provided by P.M. Pryciak), yielding the plasmid pRS316-ELM1::GFP.

pRS316-ELM1::HA$_2$. pRS316-ELM1(BamHI) was cut with BamHI and ligated to an HA$_2$ BamHI fragment, yielding the plasmid pRS316-ELM1::HA$_2$.

pRS305-CDC12. A 2μ *CDC12* plasmid was digested with PstI and XbaI to yield a 2.1 kb fragment containing the *CDC12* gene. This fragment was inserted into plasmid pRS305 (Sikorski and Hieter, 1989) digested with PstI and XbaI, yielding plasmid pRS305-CDC12. pRS305-CDC12 was cut with BstEII to target integration at the *leu2* genomic locus.

pRS305-P_{ELM1}-GFP, pRS305- P_{ELM1}-GFP-ELM1(1-640), pRS305- P_{ELM1}-GFP-ELM1(1-420), and pRS305- P_{ELM1}-GFP-ELM1(420-640). pRS316-ELM1 was used as the template in all subsquent PCR reactions unless indicated otherwise. A pRS305-P_{ELM1} plasmid was generated by cutting pRS305 with SacII and BamHI and ligated to a PCR fragment generated using the primers: 5'-AGTCAATTGCCGCGGCATTAATAC-3' and 5'-CGGTATAAGCTGTCGGGATCCCATTTCATGCTAAGT-3'. ELM1(1-640) was generated by a PCR reaction using the primers: 5'-CTTAGCATGAAATGGGATCCCGACAGCTTATACCG-3' and 5'-CTGTAGGTCGACCTATATTTGACCATTATCTGC-3'. This PCR fragment was digested with BamHI and SalI. ELM1(1-420) was generated by a PCR reaction using primers: 5'-CTTAGCATGAAATGGGATCCCGACAGCTTATACCG-3' and 5'-GTTCACCTCGAGCTATGAAATTTGACTGTGATTCCT-3'. This PCR fragment was digested with BamHI and XhoI. ELM1(420-640) was generated by a PCR reaction using the primers: 5'-ATTTCAGGATCCAGTGTGAACCCCGTAAGAAAC-3' and 5'-CTGTAGGTCGACCTATATTTGACCATTATCTGC-3'. This PCR fragment was digested with BamHI and SalI. These digested PCR fragments were ligated to pRS305-P_{ELM1} plasmid digested with appropriated restriction enzymes, resulting in pRS305-P_{ELM1}-ELM1(1-640), pRS305-P_{ELM1}-ELM1(1-420), and pRS305-P_{ELM1}-ELM1(420-640) plasmids. pRS305-P_{ELM1}, pRS305-P_{ELM1}-ELM1(1-640), pRS305-P_{ELM1}-ELM1(1-420), and pRS305-P_{ELM1}-ELM1(420-640) were digested with BamHI and ligated to a GFP BamHI fragment (kindly provided by

P.M. Pryciak), resulting in plasmids pRS305-P_{ELM1}-GFP, pRS305-P_{ELM1}-GFP-ELM1(1-640), pRS305- P_{ELM1}-GFP-ELM1(1-420), and pRS305- P_{ELM1}-GFP-ELM1(420-640).

SWE1 *deletion strains*

The plasmid pSWE1-10g (Booher et al., 1993) was cut with HindIII and BamHI and used in yeast transformations to obtain *sweΔ::LEU2* strains.

SWE1::myc13::his5$^+$ *strains*

Yeast extract preparation for immunoprecipitations

Cells were grown to exponential phase (OD_{600} ca. 0.8). For each immunoprecipitation reaction, 50 ml of yeast culture was pelleted. All subsequent manipulations were carried out at 4°C. To the cell pellet, 0.5 ml glass beads and 0.6 ml lysis buffer (50 mM Tris [pH 7.5], 1 mM EDTA, 100 mM NaCl, 0.1% NP-40, 10 mM NaF, 50 mM β-glycerolphosphate, 0.1 mM Na_3VO_4, and 1 tablet of protease cocktail [Amersham]) were added. The contents were vigorously homogenized with a multi-beadbeater (BioSpec Products) for four 1 min periods. Glass beads and cell debris were pelleted by centrifugation, and the crude extract clarified by three 10 min microfuge spins. Protein concentration of the yeast extract was measured using the Bio-Rad protein assay. Yeast extracts from

various strains were adjusted to the same protein concentration using lysis buffer.

Whole-cell lysates

1.5 ml of yeast culture at OD_{600} ca. 0.7 was pelleted and resuspended in 150 μl 1 M NaOH, 0.074% β-mercaptoethanol for 10 min at 4°C. 150 μl 50% w/v trichloroacetic acid (TCA) was added and incubated for 10 min at 4°C. The contents were spun for 2 min in a microfuge at 4°C, and the pellet was washed with 1 ml ice-cold acetone. After a short microfuge spin, acetone was removed and 150 μl of SDS-PAGE sample buffer was added. Contents were boiled for 5 min before loading on SDS-PAGE mini-gels.

Immunoprecipitation

12CA5 HA monoclonal antibody was cross-linked to protein A-Sepharose beads (Harlow and Lane, 1989) with a ratio of 2 μl antibody per 40 μl beads. 40 μl of coupled beads was added to yeast extracts of the same volume and of the same protein concentration from various strains. After incubation at 4°C with gentle shaking for 2 hours, the beads were pelleted, washed three times with lysis buffer, and resuspended in 150 μl SDS-PAGE sample buffer.

Polyacylamide gel electrophoresis and Western blotting

Samples were fractionated using 10% SDS-polyacrylamide mini-gels. Proteins were transferred to nitrocellulose filters in transfer buffer (0.2 M glycine, 0.03 M Tris, 0.1% SDS, 20% methanol). Filters were blocked for 1 hour in phosphate-buffered saline (PBS; 137 mM NaCl, 2.7 mM KCl, 8.1 mM Na_2HPO_4, 1.5 mM KH_2PO_4 [pH 7.2]) containing 0.1% Triton X-100 and 2% nonfat dry milk. 12CA5 HA monoclonal antibody (Berkeley Antibody Company), phosphotyrosine antibody (Transduction Laboratories), phospho-cdc2 antibody (kindly provided by NEB Biolabs), myc monoclonal antibody (Berkeley Antibody Company), or Ste12 antibody (kindly provided by Mary Maxon) was added at the recommended concentrations. Antigen was visualized using the Amersham ECL detection kit.

Stripping of Western blots

Filters were stripped of previously applied antibodies by immersing in stripping buffer (62.5 mM Tris [pH 6.8], 2% SDS, 100 mM β-mercaptoethanol) at 70°C for 30 min, and washed extensively in PBS.

Quantitation of Cdc28-HA tyrosine phosphorylation

To ensure that we immunoprecipited the same amount of Cdc28-HA protein, yeast extracts of the same volume and of the same protein concentration from various strains were prepared. To compare the relative amount of tyrosine phosphorylation in two strains, Cdc28-HA immunoprecipitates from strains exhibiting higher tyrosine

phosphorylation, i.e., the *elm1Δ* strain or *cdc12-6* strain, were diluted serially. The dilution that exhibited the same level of tyrosine phosphorylation with the reference, i.e., wild-type strain, determined the fold difference between the two strains.

Immunofluorescence

Immunofluorescence of yeast cells was carried out as described in Pringle et al. (1991). Cells were grown to exponential phase, fixed with 3.5% formaldehyde for 30 min, washed with PBS, and then spheroplasted. Spheroplasted cells were applied to polylysine-coated slides, submerged in -20°C methanol for 6 min and in -20°C acetone for 30 sec. Cdc3 polyclonal antibody (kindly provided by J. Frazier; Frazier et al., 1998) was used at a 1:500 dilution. Fluorescein-conjugated anti rabbit-IgG antibody was used as the secondary antibody.

Photography and image processing

An Olympus BX 65 microscope was used to visualize GFP signals and photographed with Kodak T-MAX 400 Pro film. For immunofluorescence experiments, cells were photographed with Kodak Elite II film. For morphological studies, cells were visualized with a Zeiss Axioskop and photographed with Polaroid film. Images were processed using Adobe Photoshop software.

Results

Elongated bud phenotypes of elm1 *and septin mutants require* SWE1 *function*

Several observations suggest that hyperactive *SWE1* activity leads to elongated bud phenotype. For example, cells that overexpress *SWE1* produce highly elongated buds (Booher et al., 1999; Figure 1A); the elongated-bud phenotype of mutants defective in the nim1-like kinase *HSL1* requires an intact *SWE1* gene (Ma et al., 1996; Barral et al., 1999). It has been observed that the elongated bud phenotype of *elm1* mutants is suppressed by a mutation in the *SWE1* gene, thus suggesting that *ELM1* negatively regulates *SWE1* function (Edgington et al., 1999). We set out to confirm that the behavior of *elm1* mutants is due to hyperactive *SWE1*. We carried out morphological studies to test whether the elongated-bud phenotype of *elm1* mutants requires *SWE1*. An *elm1Δ swe1Δ* strain was constructed by crossing the two single mutants. Isogenic wild-type and *swe1Δ* strains exhibited normal morphology (Figure 1B); the *elm1Δ* strain formed chains of elongated cells. In contrast, the *elm1Δ swe1Δ* strain formed cells of near wild-type morphology. These cells remained attached as in the *elm1 SWE1* strain. Thus the elongated bud phenotype of the *elm1Δ* strain requires *SWE1*.

Because septin mutants, like *elm1Δ* mutants, show an elongated-bud phenotype, they too might have increased *SWE1* activity. Indeed, it has been observed that formation of elongated cells by a *cdc12-1* strain is suppressed by deletion of *SWE1* (Barral et

al., 1999). We have tested another allele of *CDC12*, *cdc12-6*, to see whether it exhibited increased *SWE1* activity. The elongated bud phenotype of this strain was also partially suppressed by a *swe1* deletion (Figure 1C): after shift from permissive (25°C) to restrictive temperature (37°C) for two hours, cells of the *cdc12-6 swe1Δ* strain were less elongated than the *cdc12-6 SWE1* strain.

From the morphological studies, we conclude that the elongated bud phenotypes of both *elm1* and septin mutants require intact *SWE1* function.

Figure 1. Mutants overexpressing Swe1 or defective in *elm1* form elongated buds. (A) Overexpression of Swe1 leads to elongated bud formation. Wild-type strain yWW001 and strain yWW489, which contains the P_{GAL1}-*SWE1*-HA_2 plasmid, were grown in raffinose medium to exponential phase. Galactose was added to the cultures for 2 hours and cellular morphology was observed using Nomarski optics. (B) Deletion of *SWE1* suppresses the morphological defect of *elm1* mutants. Exponential-phase cultures of wild-type strain yWW001, *swe1* strain yWW305, *elm1* strain yWW274, and *elm1 swe1* strain yWW447 were examined by Nomarski optics. (C) Deletion of *SWE1* partially suppresses the morphological defect of septin mutants. Cultures of *cdc12-6* strain yWW576 and *cdc12-6 swe1* strain yWW584 were grown at 25°C to exponential phase and then shifted to 37°C for 2 hours. Cellular morphology was followed using Nomarski optics.

Figure 1

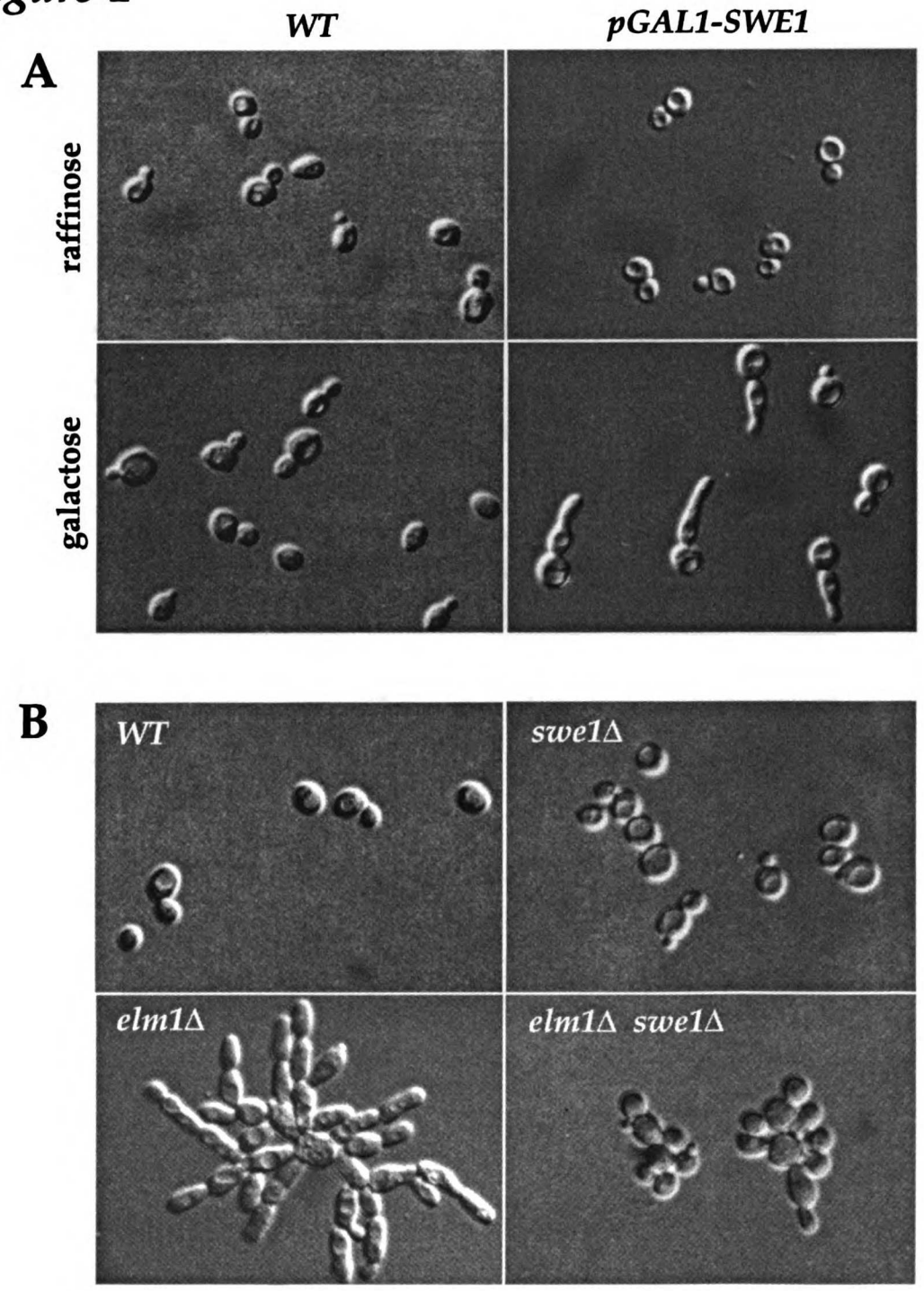
WT
pGAL1-SWE1
A
raffinose
galactose
B
WT
swe1Δ
elm1Δ
elm1Δ swe1Δ

Figure 1

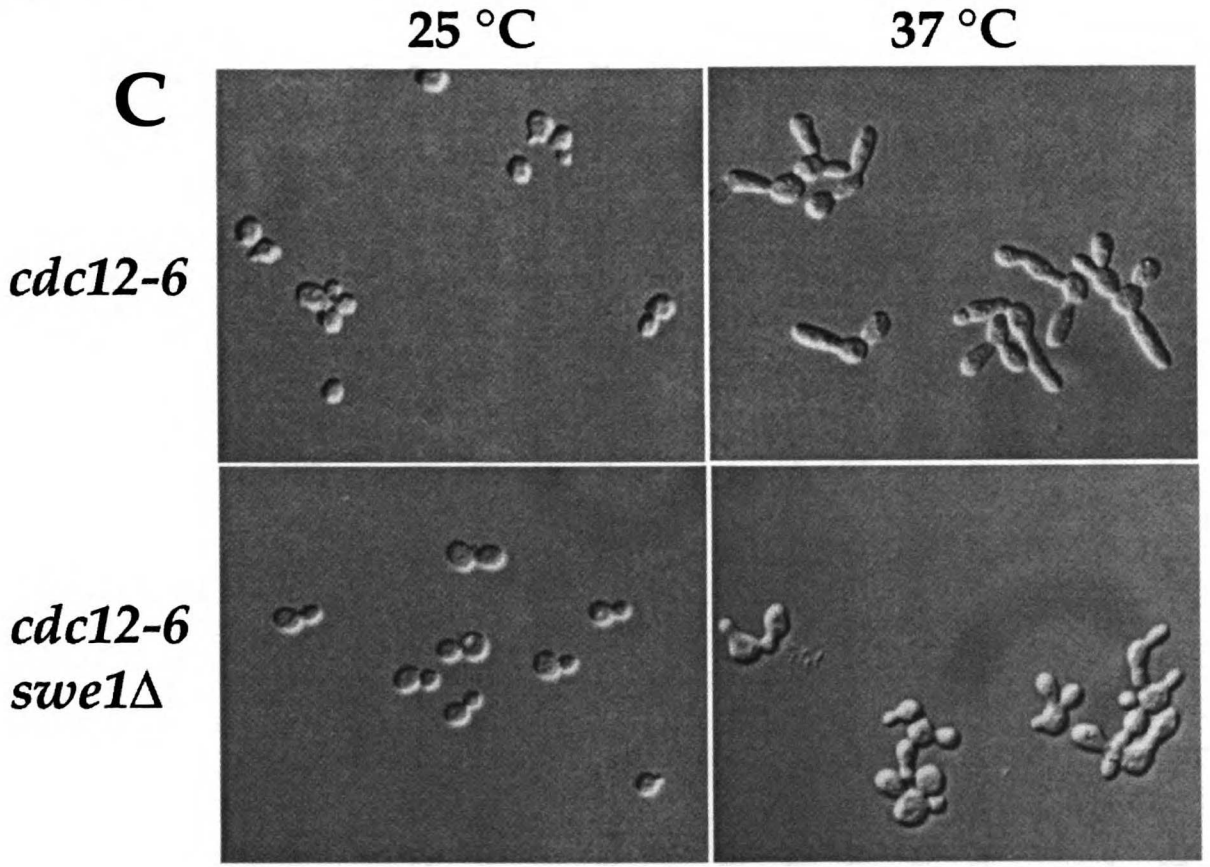

Elm1 localizes to the bud neck

Because of the dramatic morphological defect of *elm1* mutants, we suspected that Elm1 might function at specific cellular locations that are relevant to morphogenesis. In order to explore possible modes of regulation of Elm1 activity, we investigated the localization of Elm1 protein using a fusion of green fluorescent protein (Prasher et al., 1992) to the carboxyl terminus of Elm1. A low copy (*CEN-ARS*) plasmid carrying this *ELM1::GFP* fusion fully complemented the elongated bud phenotype of *elm1Δ* strains (data not shown). We observed that Elm1-GFP localized to the bud neck in cells that contain buds ranging in size from very small to large (Figure 2A). In these cells, Elm1-GFP localized as a single ring structure at the mid-point between mother and bud.

In order to facilitate visualization of the Elm1-GFP signal, we sought to observe its localization in synchronized cell populations. We therefore examined localization of Elm1-GFP in *cdc28* mutants that arrest at different stages of the cell cycle: *cdc28-13* cells arrest in G1 without DNA replication or bud formation, whereas *cdc28-1N* cells arrest in G2 with large buds and undivided nuclei (Piggott et al., 1982; Surana et al., 1991). In *cdc28-13* mutants arrested at 37°C, Elm1-GFP was not localized (<1/100); in *cdc28-1N* mutants arrested at 37°C, Elm1-GFP was localized at the bud neck in nearly every cell (93/105) (Figure 2B). Localization of Elm1 to the bud neck was confirmed using immunofluorescence of an Elm1-HA_2 fusion (see Materials and methods) expressed under control of the *ELM1* promoter on a *CEN-ARS* plasmid (data not shown).

Our data demonstrate that Elm1 kinase is localized predominantly to the bud neck.

Figure 2. Elm1 localizes to the bud neck. (A) Localization of Elm1-GFP fusion protein to the bud neck. Cultures of a wild-type strain carrying the *CEN-ARS ELM1::GFP* plasmid yWW515 were grown in SD-URA medium to exponential phase. GFP signals in living yeast cells were examined by UV-fluorescence microscopy (a). Corresponding cell morphology was followed using phase optics (b). The position of the bud neck is indicated in selected cells with an arrow. (B) Localization of Elm1-GFP fusion protein in cell cycle mutants. Cultures of *cdc28-13 elm1* and *cdc28-1N* strains harboring the *CEN-ARS ELM1::GFP* plasmid (strains yWW582 and yWW520, respectively) grown at 25°C to exponential phase were shifted to 37°C for 3 hours. Elm1-GFP localization in these arrested cells was examined by UV-fluorescence microscopy. Corresponding cell morphology was followed by Nomarski optics.

Figure 2A

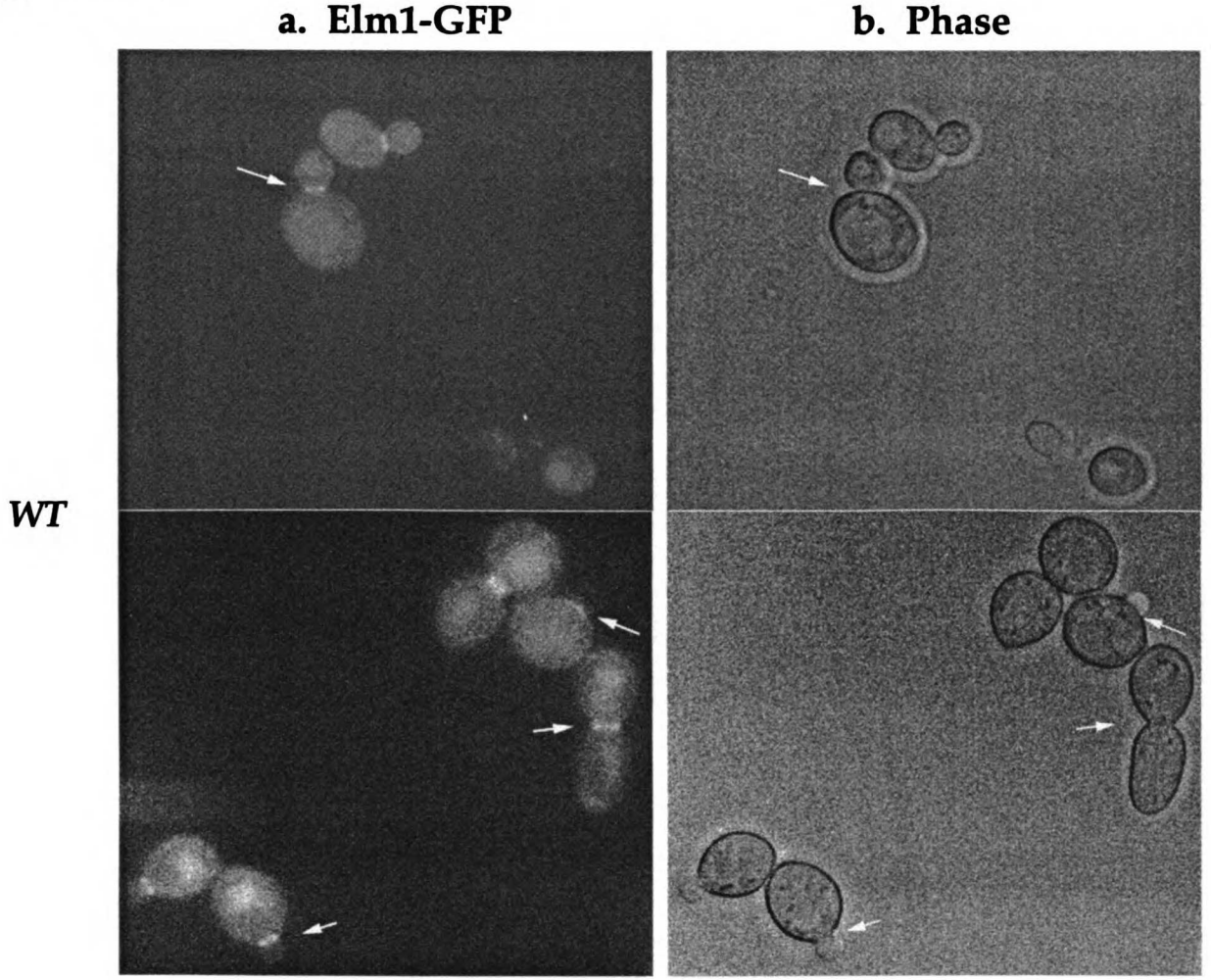

Figure 2B

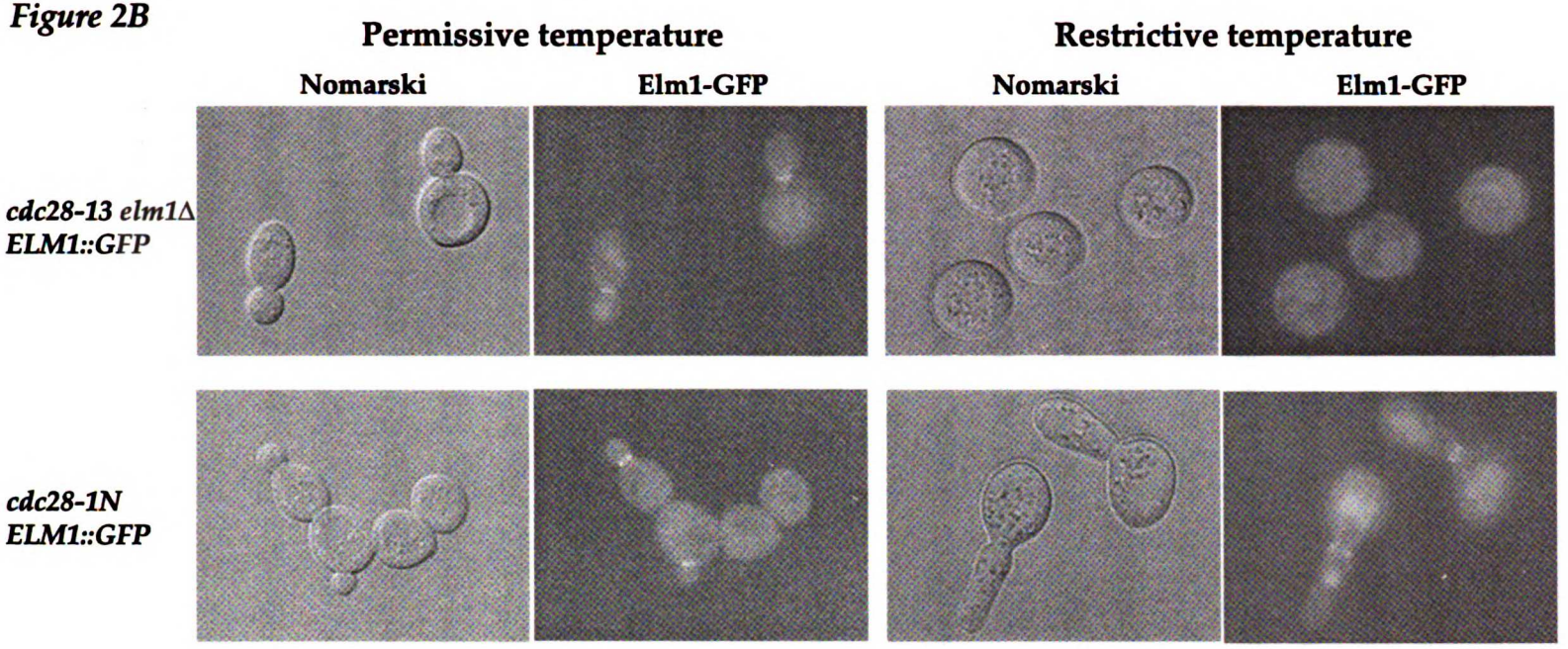
Permissive temperature
Restrictive temperature
Nomarski
Elm1-GFP
Nomarski
Elm1-GFP
cdc28-13 elm1Δ
ELM1::GFP
cdc28-1N
ELM1::GFP

Localization of Elm1 to the bud neck is dependent on the integrity of the septin ring

The localization pattern observed for Elm1 is similar to that of the septins, Cdc3, Cdc10, Cdc11, and Cdc12, which localize to the bud neck as ring structures (Haarer and Pringle, 1987; Ford and Pringle, 1991; Kim et al, 1991). Septins are required for the localization of a number of proteins to the bud neck, including Bud3, Bud4, Chs3, Myo1, Gin 4, and Hsl1 (Chant et al., 1995; Sanders and Herskowitz, 1996; DeMarini et al., 1997; Lippincott and Li, 1998; Bi et al., 1998; Longtine et al., 1998b; Barral et al., 1999). We therefore tested whether Elm1 localization also depends on the septins. The *ELM1::GFP CEN-ARS* plasmid was introduced into isogenic *cdc12-6* and *CDC12* strains, and the Elm1-GFP signal was examined after shifting cells to high temperature. Previous studies show that septins are no longer localized in *cdc12-6* mutants after shifting to the restrictive temperature for five minutes (Ford and Pringle, 1991; Kim et al., 1991; Longtine et al., 1996). We observed that the GFP signal was lost within 15 minutes after shift to high temperature and remained absent during the course of the experiment (for three hours) (Figure 3A). In contrast, Elm1-GFP was localized in the *CDC12* strain incubated at high temperature (Figure 3B and Table 2). Localization of Elm1-GFP in *cdc3*, *cdc10*, and *cdc11* mutants was similar to that in the *cdc12-6* mutant (data not shown).

In order to determine whether localization of Elm1 and septins are mutually dependent, we tested whether septin localization is affected in *elm1* mutants. In particular, we examined the localization of Cdc3 in wild-type and *elm1Δ* strains using immunofluorescence

microscopy. We found that the Cdc3 antiserum (see Materials and methods) identified a structure at the bud neck in wild-type cells as expected (Haarer and Pringle, 1987; Ford and Pringle, 1991; Kim et al, 1991). Although the morphology of *elm1* mutants is aberrant, Cdc3 protein was localized to bud neck-like constrictions in the *elm1Δ* mutant tested (Figure 3B).

We conclude that localization of Elm1 to the bud neck is dependent on septins, but not vice versa.

Figure 3. Localization of Elm1-GFP to the bud neck is septin-dependent, but not vice versa. (A) Localization of Elm1-GFP to the bud neck is dependent on the septins. Wild-type and *cdc12-6* strains containing the *ELM1::GFP* plasmid (strains yWW583 and yWW525, respectively) were grown in SD-URA medium at 25°C to log phase. Cultures were shifted to 37°C for 15 minutes. GFP signals in living yeast cells were observed by UV-fluorescence microscopy (panels a, b, c, and d). Corresponding cell morphology was followed by Nomarski optics (panels a', b', c', and d'). (B) Localization of Cdc3 to the bud neck is independent of *ELM1*. Wild-type strain yWW001 and *elm1* strain yWW274 were grown to exponential phase. The localization of Cdc3 protein was followed using immunofluorescence microscopy (a). DNA staining (b) and cell morphology (c) of the corresponding cells are shown. Arrows indicate the bud neck in selected cells.

Figure 3A

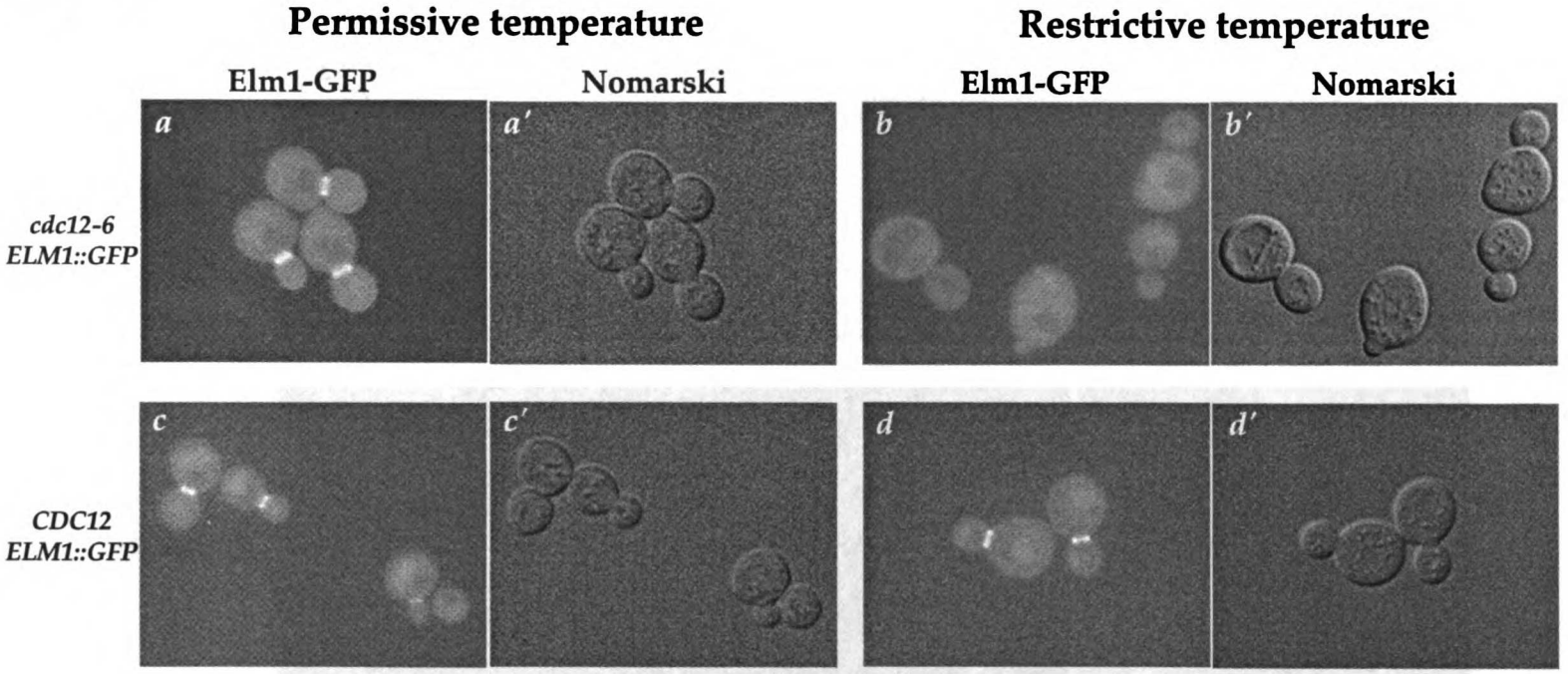
Permissive temperature
Restrictive temperature
Elm1-GFP
Nomarski
Elm1-GFP
Nomarski
a
a′
b
b′
cdc12-6
ELM1::GFP
c
c′
d
d′
CDC12
ELM1::GFP

Figure 3B

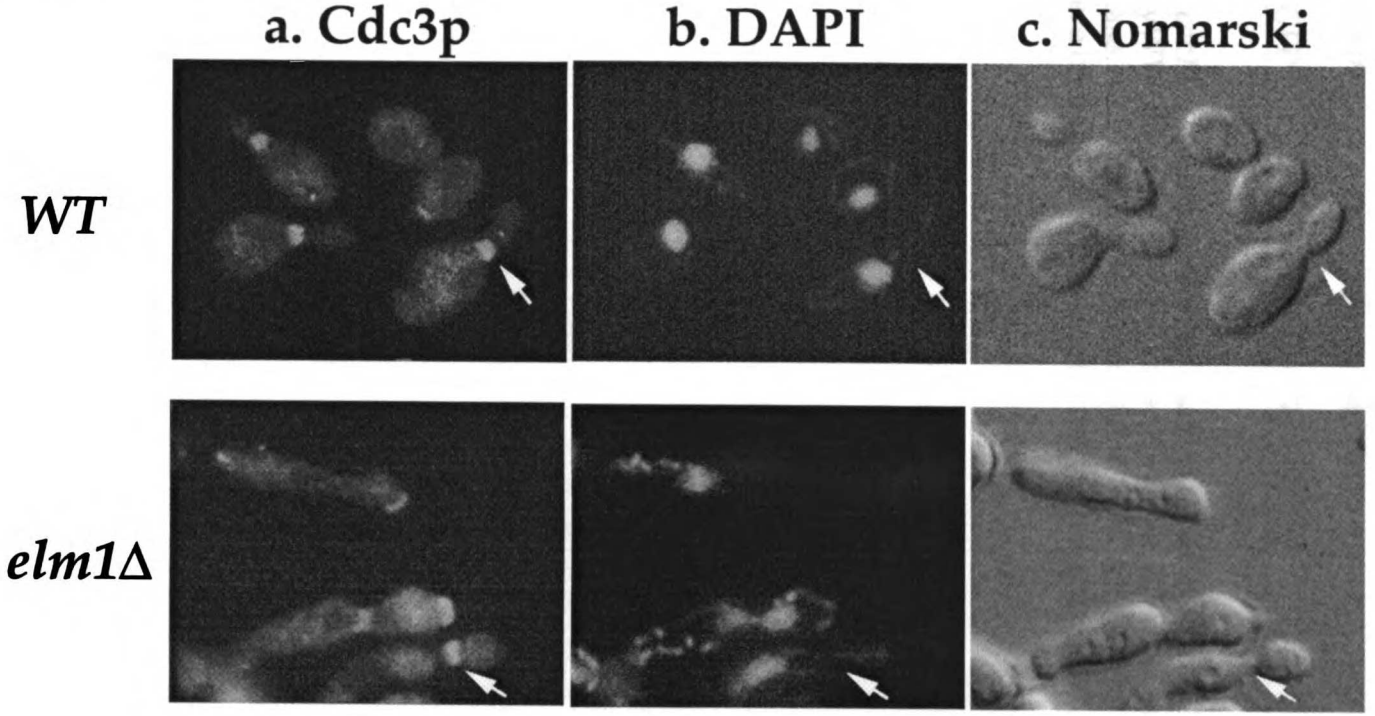

Table 2. *Localization of Elm1-GFP to the bud neck is dependent on the septin Cdc12.*

	25°C (t=0)	37°C (t=15 min)
cdc12-6 ELM1::GFP	34% (n=34/101)	<1% (n=0/100)
CDC12 ELM1::GFP	28% (n=37/133)	47% (n=47/101)

Wild-type and *cdc12-6* strains harboring the *CEN-ARS ELM1::GFP* plasmid (yWW525 and yWW583, respectively) were grown in SD-URA medium to exponential phase. The cultures were shifted to 37°C for 15 min. Cells exhibiting GFP signals were counted before and after the temperature shift.

C-terminal 220 amino acid sequence of Elm1 is necessary and sufficient for its bud neck localization

We were interested in further pursuing the element in Elm1 protein primary structure that is important for its bud neck localization pattern. Elm1 is a protein kinase of 640 amino acids and can be divided into the N-terminal kinase domain (amino acids 1-420) and the C-terminal domain (amino acids 420-640). Elm1 protein has been demonstrated to possess protein kinase activity *in vitro* (Koeler et al., 1997). Elm1 kinase domain shows low homology to the kinase domains of two other protein kinases in budding yeast, Tos3 and Pak1 (Sutherland et al., 2003; Hong et al., 2003). The C-terminal portion of Elm1 has been reported to play an auto-inhibitory role in relation to its kinase activity (Sutherland et al., 2003).

We have constructed a series of integrating plasmids that carry GFP fusions to various segments of the Elm1 protein. All fusion proteins were expressed under the transcriptional control of the *ELM1* promoter (see Material and Methods). We examined GFP signals in yeast strains carrying these plasmids (see Table 3). We found non-specific or uniform GFP localization pattern in yeast strain yWW617 expressing GFP only and in yeast strain yWW618 expressing GFP-Elm1(1-420). In contrast, GFP signals were concentrated at the bud neck in yeast strain yWW619 expressing GFP-Elm1(420-640) and in yeast strain yWW620 expressing GFP-Elm1(1-640). We therefore conclude that the C-terminal domain of Elm1 is necessary and sufficient for its bud neck localization.

We also asked whether the C-terminal bud neck localization domain of Elm1 is required for its regulation of Swe1. The

aforementioned set of plasmids was introduced into an *elm1* strain and the morphologies of the resulting strains were examined. We found that yeast strain yWW630 carrying GFP-Elm1(1-640) exhibited wild-type morphology, however, yeast strain yWW627 carrying GFP only, yeast strain yWW628 carrying GFP-Elm1(1-420), and yeast strain yWW629 carrying GFP-Elm1(420-640) exhibited elongated bud phenotype. We therefore conclude that both the kinase domain and the C-terminal bud neck localization domain are required for Elm1 function.

Table 3. *C-terminal domain of Elm is necessary and sufficient for bud neck localization.*

	GFP signal at the bud neck[a]	Rescue of *elm1* phenotype[b]
pRS305-P_{ELM1}-GFP	-	-
pRS305- P_{ELM1}-GFP-ELM1(1-640)	+	+
pRS305- P_{ELM1}-GFP-ELM1(1-420)	-	-
pRS305- P_{ELM1}-GFP-ELM1(420-640)	+	-

a. Tested in W303 *MATα* strain background.

b. Tested in W303 *MATa elm1::TRP1* strain background.

Swe1 kinase is hyperactive in septin mutants

We have observed that Swe1 kinase activity is elevated in *elm1* mutants (see Chapter 2). Because the elongated bud phenotype of septin mutants, like that of *elm1Δ* mutants, requires intact *SWE1* function, they too might have increased Swe1 kinase activity. We assayed the effect of the *cdc12-6* mutation on Swe1-dependent tyrosine phosphorylation of Cdc28. Strains grown at 25°C were shifted to 37°C for one hour and then assayed for tyrosine phosphorylation (see Material and Methods). Normalizing the amount of tyrosine phosphorylation (Figure 4A) to the amount of Cdc28 protein (Figure 4B) we observed that after one hour at restrictive temperature, tyrosine phosphorylation in *cdc12-6* mutants was three-fold that of wild-type cells (Figure 4A, lanes 2 and 4). At permissive temperature, *cdc12-6* mutants exhibited a similar amount of tyrosine phosphorylation to wild-type cells (Figure 4A, lanes 1 and 3). We confirmed that the tyrosine phosphorylation observed in the *cdc12-6* mutant strain was dependent on *SWE1* (Figure 4A, lanes 5 and 6). The *cdc12-6* mutants thus exhibited increased Swe1 kinase activity.

Based on our analysis of cell morphology and Cdc28 tyrosine phosphorylation, we conclude that Cdc12 is a negative regulator of Swe1 kinase activity.

Taken together, we conclude that *ELM1* may act in a morphogenesis checkpoint pathway that monitors that integrity of the bud neck similar to that described in Barral et al. 1999.

Figure 4. Cdc28 tyrosine 19 phosphorylation is increased in septin mutants. (A) Cultures of wild-type strain yWW586 (lane 3), *cdc12-6* strain yWW585 (lane 1), and *cdc12-6 swe1* strain yWW587 (lane 5) were grown at 25°C to early log phase and then shifted to 37°C for 1 hour (lanes 4, 2, and 6). Cdc28-HA protein was immunoprecipitated from yeast extracts and resolved by SDS-PAGE. The blot was probed with cdc2-phosphotyrosine antibody. The relative amount of tyrosine phosphorylation in each lane is indicated in arbitrary units below panel (A). (B) To normalize the amount of Cdc28 protein loaded in each lane, the western blot shown in (A) was stripped of cdc2-phosphotyrosine antibody and reprobed with 12CA5 HA antibody.

Figure 4

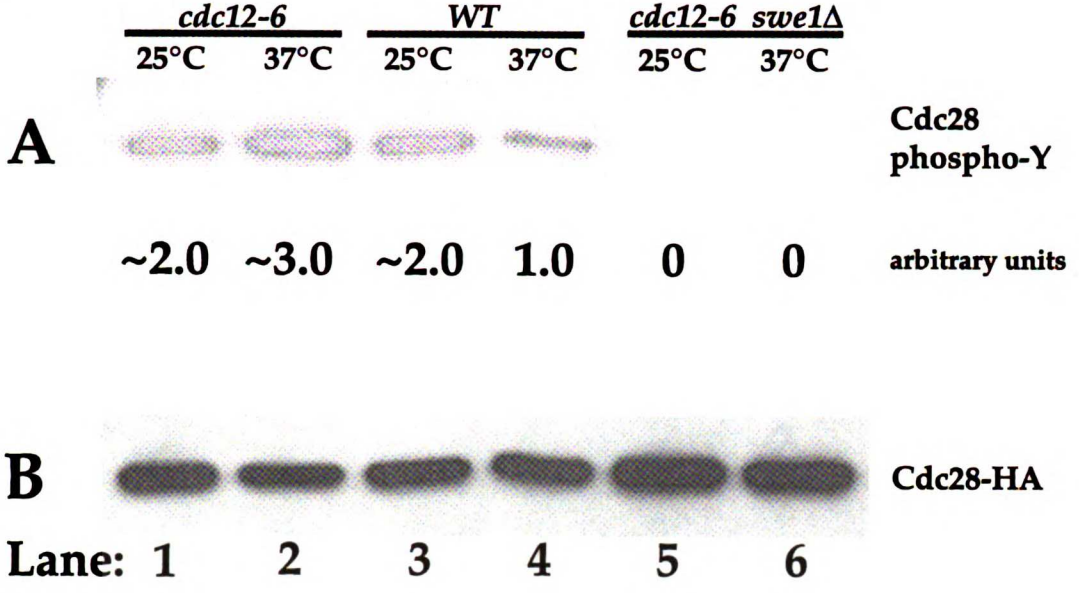
cdc12-6
WT
cdc12-6 swe1Δ
25°C
37°C
25°C
37°C
25°C
37°C
A
Cdc28
phospho-Y
~2.0
~3.0
~2.0
1.0
0
0
arbitrary units
B
Cdc28-HA
Lane: 1
2
3
4
5
6

Discussion

Increased Swe1 kinase activity in morphological mutants

Although an *elm1* mutant, the *hsl1 gin4 kcc4* triple mutant, and septin mutants do not exhibit identical phenotypes, they all form elongated buds. Furthermore, their elongated bud phenotypes are all dependent on an intact *SWE1* gene (Edgington et al., 1999; Barral et al., 1999; this study). Using phosphotyrosine and phospho-cdc2 antibodies against immunoprecipitated Cdc28, we found that Swe1 kinase activity was higher in *elm1* (see Chapter 2) and in *cdc12-6* mutants than in wild-type cells. We also observed increased Swe1 kinase activity in *hsl1* mutants using the same assay (data not shown). Whether other morphological mutants exhibit elongated buds due to hyperactive *SWE1* remains to be examined.

Functions of Elm1 and septins that are independent of SWE1

Although the elongated bud phenotype of *elm1* mutants was dependent on *SWE1*, we found that deletion of *SWE1* did not suppress the cell separation defect of *elm1* mutants (see Figure 1B). The *elm1 swe1* mutants remained attached to each other, resulting in clusters of cells, similar to those of *elm1* mutants. These observations indicate that *ELM1* has a role in cytokinesis that does not involve *SWE1*. Similarly, although a *SWE1* deletion partially suppressed the elongated bud phenotype of a *cdc12-6* strain, the *cdc12-6 swe1Δ* strain

was still temperature sensitive for growth, indicating that septins have essential functions that do not involve *SWE1*. Using an analogue-sensitive allele of *ELM1*, it has been demonstrated that inhibition of Elm1 kinase activity leads to a delay in bud emergence. This observation suggests a role of Swe1 in early G1 phase unrelated to its function in the regulation of Swe1 (Sreenivasan and Kellogg, 2003). Elm1 may also function as an upstream activating kinase in the regulation of the SNF1 complex in response to metabolic stress in budding yeast (Sutherland et al., 2003; Hong et al., 2003).

Localization of Elm1 and nim1-related kinases to the bud neck

Since our study of Elm1 localization in budding yeast, a number of other labs have published their observations confirming our data (Moriya and Isono, 1999; Bouquin et al., 2000; Thomas et al., 2003). It is striking to note that the nim1-related protein kinases have also been localized to the bud neck (Okuzaki et al., 1997) and that their localizations are also septin-dependent (Longtine et al., 1998b; Barral et al., 1999), suggesting that Elm1 and the nim1-related kinases may have direct interactions. Indeed, it has been proposed that Elm1 act upstream of Hsl1 in the regulation of Swe1 (Edgington et al., 1999). However, a model in which Elm1 and Hsl1 act independently to regulate Swe1 cannot be excluded. The localization of Elm1 and nim1-related kinases to the bud neck is somewhat different: we found Elm1-GFP localized as a single ring at the mid-point between the mother and the bud, whereas nim1-related kinases localize as

double rings at the neck region (Longtine et al., 1998b; Barral et al., 1999). The difference in localization of Elm1-GFP and the nim1-related kinases does not appear to be due to a difference in procedures used for localization, as we have observed that Hsl1-GFP formed double rings at the bud neck (data not shown).

Localization of Elm1 to the bud neck may be important for the function of Elm1 in a couple of ways: Elm1 kinase activity may require bud neck localization in order to be activated; or localization to the bud neck may provide a physical site for Elm1 to interact with its substrates. We have found that the C-terminal domain of Elm1 is necessary and sufficient for Elm1 to localize to the bud neck. It has been suggested that the C-terminal domain is auto-inhibitory to the kinase activity of Elm1 (Sutherland et al., 2003). It is thus tempting to suggest that Elm1 localize to the bud neck via its C-terminal domain, releasing the kinase domain, permitting the activation of the kinase activity.

Regulation of Elm1 by the septins

Suppression of the elongated-bud phenotype of *elm1* and septin mutants by a *SWE1* deletion suggests that *ELM1* and the septins possibly act in the same pathway that leads to the inhibition of Swe1 activity. Indeed, we found that Elm1 was localized to the bud neck and that this localization was dependent on the septins. The fact that Elm1 localization to the bud neck was disrupted within fifteen minutes after shifting to restrictive temperature suggests that the interaction between Elm1 and the septins may be direct. The

mechanism by which the septins regulate Elm1 remains to be determined. It is possible that the septin complex is required for the activation of Elm1 kinase activity or that septins simply provide the platform for Elm1 to interact with its substrates.

The Elm1-Swe1 pathway may function in the switch from apical to isotropic bud growth

To produce an ovoid cell shape, cells must switch from apical to isotropic bud growth at a certain point after the G1/S transition. Our data support the hypothesis that the bud neck is the cellular structure that initiates the signal for the morphogenetic switch (Barral et al., 1999). Appearance of the bud neck at the G1/S transition provides an obvious landmark event to indicate that a cell has committed to cell division. The bud neck also serves as the site of cytokinesis at the end of mitosis. Different sets of proteins are likely to be localized to the bud neck at different stages of the cell cycle to accomplish different tasks. Transcription of the *ELM1* gene has been shown to peak in the G2 phase of the cell cycle (Cho et al., 1998; Spellman et al., 1998). It is possible that accumulation of Elm1 and other proteins at the bud neck in G2 may be the signal for the morphogenetic switch (see Figure 5). The septins therefore play an important role in this signal pathway as the structural component of the bud neck.

Figure 5. A model for the signal transduction pathway from the septins to Cdc28 that results in the morphogenetic switch. In budding yeast, Cln/Cdc28 activity promotes bud formation and apical bud growth, whereas Clb/Cdc28 activity promotes isotropic bud growth (Lew and Reed, 1993). Localization of Elm1 and the nim1-related protein kinases to the bud neck leads to the inhibition of Swe1 kinase activity, resulting in the activation of the Clb/Cdc28 kinase activity (see also Barral et al., 1999). The growth of the bud is switched to the isotropic mode in order to produce the ovoid shape of a yeast cell. In addition to participating in the Swe1-dependent morphogenetic switch, Elm1 and the septins also play a role in cytokinesis that is independent of Swe1.

Figure 5

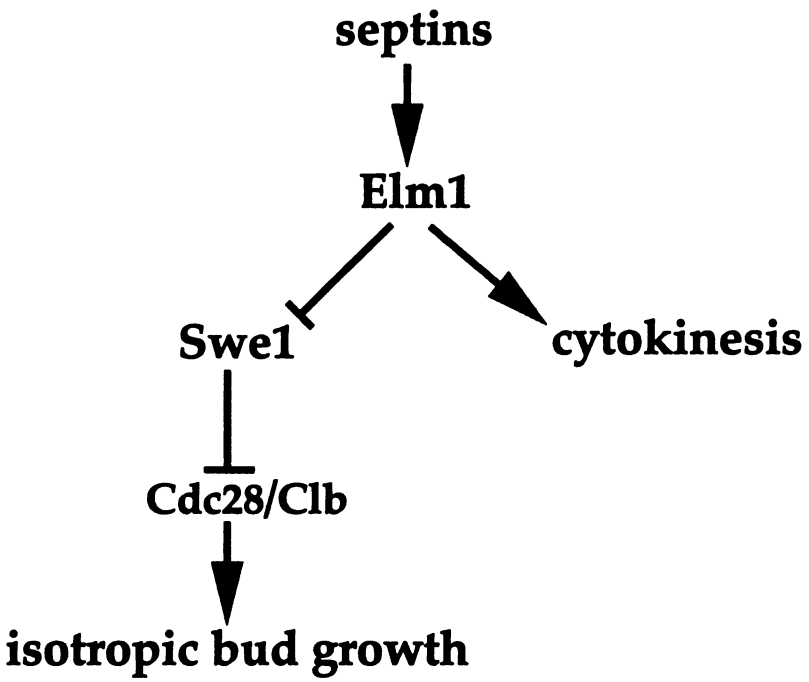
septins
Elm1
Swe1
cytokinesis
Cdc28/Clb
isotropic bud growth

References

Barral, Y., M. Parra, S. Bidlingmaier, and M. Snyder. 1999. Nim1-related kinases coordinate cell cycle progression with the organization of the peripheral cytoskeleton in yeast. *Genes & Dev.* **13**: 176-187.

Bi, E., P. Maddox, D.J. Lew, E.D. Salmon, J.N. McMillan, E. Yeh, and J.R. Pringle. 1998. Involvement of an actomyosin contractile ring in *Saccharomyces cerevisiae* cytokinesis. *J. Cell Biol.* **142**: 1301-1312.

Booher, R.N., R.J. Deshaies, and M.W. Kirschner. 1993. Properties of *Saccharomyces cerevisiae* wee1 and its differential regulation of $p34^{CDC28}$ in response to G1 and G2 cyclins. *EMBO J.* **12**: 3417-3426.

Bouquin, N., Y. Barral, R. Courbyrette, M. Blondel, M, Snyder, and C. Mann. 2000. Regulation of cytokinesis by the Elm1 protein kinase in *Saccharomyces cerevisiae*. *J. Cell Sci.* **113**: 1435-1445.

Byers, B. and L. Goetsch. 1976. A highly ordered ring of membrane associated filaments in budding yeast. *J. Cell Biol.* **69**: 717-721.

Chant, J., M. Mischke, E. Mitchell, I. Herskowitz, and J. R. Pringle. 1995. Role of Bud3p in producing the axial budding pattern of yeast. *J. Cell Biol.* **129**: 767-778.

Cho, R.J., M.J. Campbell, E.A. Winzeler, L. Steinmetz, A. Conway, L. Wodicka, T.G. Wolfsberg, A.E. Gabrielian, D. Landsman, D.J. Lockhart, and R.W. Davis. 1998. A genome-wide transcriptional analysis of the mitotic cell cycle. *Mol. Cell* **2**: 65-73.

DeMarini, D.J., A.E.M. Adams, H. Fares, C. De Virgilio, G. Valle, J.S. Chuang, and J.R. Pringle. 1997. A septin-based hierarchy of proteins required for localized deposition of chitin in the *Saccharomyces cerevisiae* cell wall. *J. Cell Biol.* **139**: 75-93.

Edgington, N. P., M. J. Blacketer, T. A. Bierwagen, and A. M. Myers. 1999. Control of *Saccharomyces cerevisiae* filamentous growth by cyclin-dependent kinase Cdc28. *Mol. Cell. Biol.* **19**: 1369-1380.

Ford, S.K. and J.R. Pringle. 1991. Cellular morphogenesis in the *Saccharomyces cerevisiae* cell cycle: localization of the *CDC11* gene product and the timing of events at the budding site. *Dev. Genet.* **12:** 281-292.

Frazier, J.A., M.L. Wong, M.S. Longtine, J.R. Pringle, M. Mann, T.J. Mitchison, and C. Field. 1998. Polymerization of purified yeast septins: evidence that organized filament arrays may not be required for septin function. *J. Cell Biol.* **143**: 737-749.

Guthrie, C. and G.R. Fink. 1991. Guide to yeast genetics and molecular biology. *Meth. Enzymol.* **194**: 1-933.

Haarer, B.K. and J.R. Pringle. 1987. Immunofluorescence localization of the *Saccharomyces cerevisiae CDC12* gene product to the vicinity of the 10-nm filaments in the mother-bud neck. *Mol. Cell. Biol.* **7**: 3678-3687.

Hartwell, L.H. 1971. Genetic control of the cell division cycle in yeast. IV. Genes controlling bud emergence and cytokinesis. *Exp Cell Res.* **69**: 265-76.

Hartwell, L.H., R.K. Mortimer, J. Culotti, and M. Culotti. 1973. Genetic Control of the Cell Division Cycle in Yeast: V. Genetic Analysis of cdc Mutants. *Genetics* **74**: 267-286.

Hong S.P., F.C. Leiper, A. Woods, D. Carling, and M. Carlson. 2003. Activation of yeast Snf1 and mammalian AMP-activated protein kinase by upstream kinases. *Proc. Natl. Acad. Sci.* **100:** 8839-8843.

Kim, H.B., B.K. Haarer, and J.R. Pringle. 1991. Cellular morphogenesis in the *Saccharomyces cerevisiae* cell cycle: localization of the *CDC3* gene product and the timing of events at the budding site. *J. Cell Biol.* **112**: 535-544.

Koehler, C.M. and A.M. Myers. 1997. Serine-threonine protein kinase activity of Elm1p, a regulator of morphologic differentiation in *Saccharomyces cerevisiae. FEBS Letters* **408**: 109-114.

Lew, D.J. and S.I. Reed. 1995. A cell cycle checkpoint monitors cell morphogenesis in budding yeast. *J. Cell Biol.* **129**: 739-749.

Li, R. and A.W. Murray. 1991. Feedback control of mitosis in budding yeast. *Cell* **66**: 519-31.

Lippincott, J. and R. Li. 1998. Sequential assembly of myosin II, an IQGAP-like protein, and filamentous actin to a ring structure involved in budding yeast cytokinesis. J. Cell Biol. 140: 355-366.

Longtine, M.S., D.J. DeMarini, M.L. Valencik, O.S. Al-Awar, H. Fares, C. De Virgilio, and J.R. Pringle. 1996. The septins: roles in cytokinesis and other processes. *Curr. Opin. Cell Biol.* **8**: 106-119.

Longtine, M.S., H. Fares, and J.R. Pringle. 1998. Role of the yeast Gin4p and the relationship between septin assembly and septin function. *J. Cell Biol.* **143**: 719-736.

Longtine, M.S., C.L. Theesfeld, J.N. McMillan, E. Weaver, J.R. Pringle, and D.J. Lew. 2000. Septin-dependent assembly of a cell cycle-regulatory module in *Saccharomyces cerevisiae*. *Mol. Cell. Biol.* **20**: 4049-61.

Ma, X.-J., Q. Lu, and M. Grunstein. 1996. A search for proteins that interact genetically with histone H3 and H4 amino termini uncovers novel regulators of the Swe1 kinase in *Saccharomyces cerevisiae*. *Genes & Dev.* **10**: 1327-1340.

Moriya H. and K. Isono. 1999. Analysis of genetic interactions between *DHH1*, *SSD1* and *ELM1* indicates their involvement in

cellular morphology determination in *Saccharomyces cerevisiae*. *Yeast* **15**: 481-96.

Okuzaki, D., S. Tanaka, H. Kanazawa, and H. Nojima. 1997. Gin4 of *S. cerevisiae* is a bud neck protein that interacts with the Cdc28 complex. *Genes Cells.* **2**: 753-770.

Piggott, J.R., R. Rai, and B.L. Carter. 1982. A bifunctional gene product involved in two phases of the yeast cell cycle. *Nature* **298**: 391-393.

Prasher, D.C., V.K. Eckenrode, W.W. Ward, F.G. Prendergast, and M.J. Cormier. 1992. Primary structure of the *Aequorea victoria* green-fluorescent protein. *Gene* **111**: 229-33.

Pringle, J.R., A.E.M. Adams, D.G. Drubin, and B.K. Haarer. 1991. Immunofluorescence methods for yeast. *Meth. Enzymol.* **194**: 565-602.

Sambrook, J., E.F. Fritsch, and T. Maniatis. 1989. Molecular Cloning: A Laboratory Manual. 2nd ed. Cold Spring Harbor Laboratory Press, Cold Spring Harbor, NY.

Sanders, S.L. and I. Herskowitz. 1996. The Bud4 protein of yeast, required for axial budding, is localized to the mother/bud neck in a cell cycle-dependent manner. *J. Cell Biol.* **134**: 413-427.

Sikorski, R.S. and P. Hieter. 1989. A system of shuttle vectors and yeast host strains designed for efficient manipulation of DNA *in Saccharomyces cerevisiae*. *Genetics* **122**: 19-27.

Spellman, P.T., G. Sherlock, M.Q. Zhang, V.R. Iyer, K. Anders, M.B. Eisen, P.O. Brown, D. Botstein, and B. Futcher. 1998. Comprehensive identification of cell cycle-regulated genes of the yeast *Saccharomyces cerevisiae* by microarray hybridization. *Mol. Biol. Cell* **9**: 3273-3297.

Sreenivasan, A, A.C. Bishop, K.M. Shokat, and D.R. Kellogg. 2003. Specific inhibition of Elm1 kinase activity reveals functions required for early G1 events. *Mol. Cell. Biol.* **23:** 6327-37.

Surana, U., H. Robitsch, C. Price, T. Schuster, I. Fitch, A.B. Futcher, and K. Nasmyth. 1991. The role of *CDC28* and cyclins during mitosis in the budding yeast *S. cerevisiae*. *Cell* **65**: 145-61.

Sutherland, C.M., S.A. Hawley, R.R. McCartney, A. Leech, M.J. Stark, M.C. Schmidt, and D.G. Hardie. 2003. Elm1p is one of three upstream kinases for the Saccharomyces cerevisiae SNF1 complex. *Curr Biol.* **13:**1299-305.

Thomas, C.L., M.J. Blacketer, N.P. Edgington, and A.M. Myers. 2003. Assembly interdependence among the *S. cerevisiae* bud neck ring proteins Elm1p, Hsl1p and Cdc12p. *Yeast* **20**: 813-26.


UC
San Francisco
LIBRARY
UNIVERSITY OF CALIFORNIA · UNIVERSITY OF CALIFORNIA

7271789
3 1378 00727 1789
For reference
Not to be taken from the room.